CONTROLLED SIZE MTT (ZSM-23) ZEOLITES FOR CATALYTIC CRACKING

BY

IDRIS AKOLADE BAKARE

A Thesis Presented to the
DEANSHIP OF GRADUATE STUDIES

KING FAHD UNIVERSITY OF PETROLEUM & MINERALS

DHAHRAN, SAUDI ARABIA

In Partial Fulfillment of the
Requirements for the Degree of

MASTER OF SCIENCE

In

CHEMICAL ENGINEERING

DECEMBER 2012

KING FAHD UNIVERSITY OF PETROLEUM & MINERALS

DHAHRAN- 31261, SAUDI ARABIA

DEANSHIP OF GRADUATE STUDIES

This thesis, written by **IDRIS AKOLADE BAKARE** under the direction his thesis advisor and approved by his thesis committee, has been presented and accepted by the Dean of Graduate Studies, in partial fulfillment of the requirements for the degree of **MASTER OF SCIENCE IN CHEMICAL ENGINEERING.**

A. Al Amer

Dr. Adnan M. Jarallah Al-Amer
(Advisor)

Dr. Usamah A. Al-Mubaiyedh
Department Chairman

Che Muraza

Dr. Oki Muraza
(Co-Advisor)

Dr. Salam A. Zummo
Dean of Graduate Studies

Mozahar Hossain

Dr. Mohammad Mozahar Hossain
(Member)

5/2/13

Date

Dr. Zuhair

Dr. Zuhair Omar Malaibari
(Member)

Shaikh Abdur Razzak

Dr. Shaikh Abdur Razzak
(Member)

[6T]

This work is dedicated to almighty Allah for His mercy and guidance from the day I step foot on earth till the day I will return to Him. I thank Him and glorify Him for he who is grateful to his lord will get more favors in abundance.

ACKNOWLEDGMENTS

ALHAMDULILLAH, all praises are due to Allah, the Most Beneficent the Most Merciful. I exonerate Him for the mercy and opportunity He bestowed on me to complete this Masters of Science program and research work.

Thereafter, I acknowledge King Fahd University of Petroleum and Minerals for giving me the opportunity to undertake this graduate studies program.

My profound gratitude goes to my proficient and patient supervisors, Dr Adnan M. Jarallah Al-Amer and Dr Oki Muraza for their endless support in seeing me through with this work. And to my committee members Dr Mohammed Mozahar Hussain, Dr Zuhair Omar Malaibari and Dr Shaikh Abdur Razzak I deeply appreciate their contributions.

My sincere appreciation also goes to the Chairman of Chemical Engineering Department Dr. Usamah A. Al-Mubaiyedh and the entire faculty and staff. Also to my friends and the entire Nigerian community I thank you all for your support.

My earnest gratitude also goes to the Director, Dr Zain H. Yamani and all the scientist of the center of nanotechnology (CENT) for their support through my research. I am indeed grateful.

And not forgetting my mother and father, I immensely appreciate their care from scratch till date. I pray Allah in His infinite mercy bless them and be merciful unto them as they have nurtured me with love since I was a baby.

To my siblings and in-laws, your unending support is duly acknowledged. I pray Allah's mercy be with you all.

To my darling wife Hadiza Sarumoh Bakare, to the world you might be just one person but to me you are the world. Thank you for your undying love, care, forbearance and support all through the way. And to our unborn kids who will grace our world with us inshallah. I love you all more than words can express.

And to all well wishers, thank you all and I wish you all the best.

TABLE OF CONTENTS

LIST OF TABLES

LIST OF FIGURES

LIST OF ABBREVIATION

ANOVA	: Analysis of Variance
BET	: Brunauer Emmett Teller
BTX	: Benzene Toluene Xylene
EDX	: Energy Dispersive X-ray
DMF	: N N-dimethylformamide
DOE	: Design of Experiment
FAU	: Faujasite
FESEM	: Field Emission Scanning Electron Microscope
LTA	: Linde type A
LTL	: Linde type l
MFI	: Mordenite Framework Inverted
MTT	: Mobil Twenty Three
NMR	: Nuclear Magnetic Resonance
OA	: Orthogonal Array
OSDA	: Organic Structural Directing Agent
P/E	: Propylene to ethylene ratio
R-H	: Rice-Herzfeld

R-K : Rice Kossiakoff

S/N : Signal to noise ratio

TON : Theta One

XRD : X-ray Diffraction

XRF : X-ray fluorescence

ZSM : Zeolite Socony Mobil

ABSTRACT

Full Name : [Idris Akolade Bakare]

Thesis Title : [Controlled MTT zeolites for Catalytic cracking]

Major Field : [Chemical Engineering]

Date of Degree : [December 2012]

Due to the rise in demand and price of propylene over ethylene, the need to increase the selective production of propylene is necessary. Our study focuses on developing a one dimensional zeolite which is suitable for the selective cracking of light naphtha (using n-hexane as a model reactant) to produce propylene. In order to achieve this, we studied the effect of the incorporation of a nonionic surfactant in the synthesis of Mobil Twenty Three (MTT) zeolite, a one –dimensional 10-membered ring (10 MR) zeolite via a microwave reactor. Incorporation of nonionic polyoxyethylene 20 stearyl ether (Brij-78) surfactant into a synthesis mixture of SiO_2-Al_2O_3 - NaOH- Brij-78 - isopropyl amine - H_2O at different Brij-78/SiO_2 ratio (0, 0.04 and 0.07) was studied with different synthesis aging time of 5, 24 and 48 h. The Taguchi method and the Pareto Analysis of variance were used to investigate the effects of Brij-78/SiO_2 ratio and synthesis aging time on as-synthesized samples Brunauer Emmett Teller (BET) surface area and mean crystal length. In order to minimize diffusion and mass transfer problems in our catalyst, we focused on minimizing catalyst mean crystal length and maximizing catalyst BET surface area. Characterization techniques such as X-ray diffraction (XRD), BET, Field Emission Scanning Electron Microscope FESEM, energy dispersive X-ray (EDX) and twenty seven aluminum nuclear magnetic resonance (^{27}Al NMR) were used. Pure Rod-like MTT zeolite phase were obtained with crystal length in the submicron to nanometer range.

Both Taguchi and Pareto analysis show that aging time of synthesis precursor is more significant with minimal competition from Brij-78/SiO_2 ratio in reducing mean crystal length and increasing BET surface area of catalyst. Catalytic test of MTT zeolite in the cracking of n-hexane shows good selectivity and yield towards olefins. Also, Propylene to ethylene ratio (P/E) of ~2.5 was recorded for evaluated catalyst. Furthermore, increase in catalyst activity and resistance to deactivation was observed after desilication followed by mild dealumination.

ملخص الرسالة

الاسم الكامل: ادريس أكوليد بكارى

عنوان الرسالة: MTT زيولايت للرقابة لتكسير بالوسيط الكيميائي

التخصص: الهندسة الكيميائية

تاريخ الدرجة العلمية: ديسمبر ٢٠٢١

إنتاج مادة البروبلين أصبح حاجة ماسة وذلك نظراً للزيادة في الإحتياج العالمي مقارنة بـ الإيثلين. ركزت هذه الدراسة على تطوير مادة حفازة من نوع الزيولايت احادي البعد وذلك لإنتاج البروبلين بواسطة التكسير الحفزي للنفثا الخفيفة، وقد استعمل الهكسان كممثل للنفثا. لتحقيق هذا الغرض تم تطوير المادة الحفزية MTT وذلك بإدخال مواد رابطة غير أيونية عن طريق عملية تحضير في مفاعل باستخدام الميكروويف. تمت دراسة عملية التحضير تحت ظروف زمنية مختلفة وذلك تحت الفترات 5 ساعات 24 ساعة و 48 ساعة. دراسة فترات التحضير الزمنية بالإضافة إلى نسبة المادتين SiO_2 و Brij المستعملتان في عملية التحضير تم عن طريق عملية تحليل احصائي وهي Taguchi and Pareto Analysis على مساحة السطح BET وطول الكرستالات لقد وجدت هذه الدراسة الإحصائية أن التأثير الأعلى لفترة التحضير الزمنية يكون عندما تكون نسب المواد SiO_2 و Brij قليلة. وعند هذه الظروف يتم الحصول على مساحة سطح BET أعلى وطول أقل لكرستالات المادة الحفزية. وهذه هي الظروف الملائمة لزيادة فعالية المادة الحفزية. حيث وجدت هذه الدراسة أن تحضير المادة الحفزية MTT تحت هذه الظروف أدى إلى إنتاج

نسب أعلى من الألكينات وهو المطلوب لزيادة إنتاج مادة البروبلين والذي كان هدف هذه الدراسة.

CHAPTER 1

INTRODUCTION

Continuous quests to develop better catalytic processes in chemical industries, among others, depend on finding the best catalysts with optimized catalyst properties and process conditions. Solid acid catalysts such as zeolites are used in many of the petrochemical processes to obtain basic chemicals such as olefins and benzene-toluene-xylene (BTX) derivatives [1]

One-dimensional pore zeolites have been studied extensively in typical shape-selective petrochemical industrial reactions [2-5]. MTT zeolite is one-dimensional pore zeolite with pore diameter of 0.45 nm × 0.52 nm, which is smaller than that of ZSM-5 [6]. Its unique pore structure has made it suitable in various reactions like the selective isomerization of butane and catalytic cracking of C4 alkenes to ethylene and propylene[7].

MTT zeolite is a one-dimensional zeolite that grows as bundles of needles of approximately 10 μm in length [8]. Due to the lengthy needle-like nature possessed by MTT zeolite, the coking rate in reactions such as catalytic cracking of hydrocarbons is fast. The high coking rate is due to pore blocking of zeolite pores, which in turns reduces mass transfer of reactants into zeolites pore where active sites are present. Thus, in order to improve mass transfer of reactants or

products, catalyst stability and activity of catalyst, facile tuning of zeolite (morphology) is required.

Enormous effort has been invested [9] in tuning the shape and size of one dimensional pore zeolites. Studies have shown that changing synthesis parameters such as silica to water ratio [10], amount hydroxyl ion from base (example, NaOH), use of co-solvent [11], and implementation of crystal growth inhibitors [12] has great effect on the shape and size of one dimensional pore zeolites. All of these efforts are aimed at getting improved catalyst for various industrial purposes.

Nonionic surfactants coupled with co-solvents like cyclohexane and hexane have been extensively used in improving the surface and catalytic properties of zeolites in order to improve their catalytic properties [9]. Extensive studies have shown that to extract the best capability of a catalyst, careful modification of synthesis parameters is needed. Therefore, in order to improve the catalytic properties of our zeolite of interest, MTT zeolite, we seek means of carefully adjusting synthesis parameters (aging time and Brij-78 surfactant concentration) aided with optimization techniques (Taguchi analysis and Pareto analysis of variance). Thereafter, catalytic cracking of n-hexane is used as a model reaction to measure activity of synthesized catalyst.

1.1 OBJECTIVES OF STUDY

Our aim is to develop an improved MTT zeolite for selective cracking of n-hexane to propylene. In order to achieve this goal, the synergic effects of both nonionic surfactants and co-solvent have been extensively studied. In the light of these, our studies were focused on the following tasks:

- The effect of incorporation of nonionic surfactant in the growth of MTT zeolite implementing Taguchi L9 orthogonal method and Pareto ANOVA.
- The effect of simultaneous desilication and dealumination on as synthesized samples.
- Characterization of as synthesized samples using Energy Dispersive X-ray Analysis (EDX), Nuclear Magnetic Resonance (NMR), Brunauer-Emmett-Teller (BET), Field Emission Scanning Electron Microscope (FESEM), and X-ray diffraction (XRD).
- Catalytic testing and deactivation study of as synthesized samples in the cracking of n-hexane.

CHAPTER 2

LITERATURE REVIEW

2.1 One Dimensional pore zeolites

Most of the zeolite catalysts known and used in the petrochemical industries have three dimensional (3D) pore connection such as Mordenite framework inverted (MFI) and Faujasite (FAU) [13].However, the less investigated one-dimensional pore zeolites also have the potential of being employed in the petrochemical industries. The likes of these zeolites are ZSM-22, Mordenite (MOR), and ZSM-23 (MTT) and many others.

ZSM-22 (Theta one (TON))belongs to the class of medium pore zeolites such as ZSM-5, ZSM-11 and ZSM-35 with one dimensional 10 member ring (MR) opening belonging to 0.55 nm X 0.45 nm [14, 15]. Due to its structure and acidity it has been used in various reactions like the skeletal isomerization of n-butene [16], hydrocracking and isomerization of n-paraffin mixtures [17].

Modernite (MOR) constitute a micro-pore with two pore-channels, an elliptical pore channel (0.67 – 0.7 nm) which runs parallel to the c-axis and, and another pore channel which runs parallel to the b-axis (0.26 -0.57 nm) [18]. Due to high thermal stability and acidity it is being used in isomerization [19], reforming [20] and alkylation[21].

2.2. Size and shape control of zeolite catalysts

The unique pore system of zeolite crystals have made them well known as size and shape selective catalyst. This ability helps to improve selectivity of desired products in certain chemical reaction where the desired product is highly favored by the pore of the zeolite catalyst. Most one dimensional pore zeolites are shape selective catalyst and have found many uses in various reactions. The excellent shape selective ability of zeolites in hydrogenation and hydrogen transfer reactions reviewed elsewhere [4] further affirms this claim.

2.3. MTT zeolites as shape-selective catalysts

ZSM-23 a medium pore zeolite rich in silica with MTT topology was first developed by Plank et al [22] at Mobil in 1978. Its framework consists of 5, 6 and 10 member rings with no intersecting channels and tear drop pore with diameter 0.52 x 0.45nm[6]. Table 2.1 gives a summary of various templates used in the synthesis of ZSM-23 zeolite.

Owing to the unique one dimensional 10 member ring structure and acidities of ZSM-23, excellent catalytic activity and shape selectivity have been reported for the hydroisomerization of the long-chain paraffin [23, 24] and isomerization of xylene [25]. Table 2.2 shows various reaction schemes in which ZSM-23 has been employed.

Table 2.1 Different template for the synthesis of ZSM-23.

SDA:Structure-directing agent	SiO_2/Al_2O_3 Ratio	T [^oC]	t (h)	H_2O/Si	OSDA/Si	Reference
Isopropyl amine	60 – 150	170	72	12	0-1.2	[26]
N,N-dimethylformamide (DMF)	30-300	160-200	48-480	45	3-10	[7]
Pyrrolidine	50-220	138-204	6-336	30	0.7-2.8	[22]

Table 2.2 Different applications of ZSM-23.

Reaction Scheme	**Reference**
Bifunctional catalytic isomerization of decane	[23]
Isomerization and formation of xylenes	[25]
Catalytic cracking of C4 alkenes	[27]
Catalytic cracking of C4 alkanes	[28]
Alkylation of aromatic hydrocarbons	[29]

2.4. Microwave synthesis of zeolites

Recently, microwave irradiation as method of synthesizing zeolites has been widely used recently to rapidly synthesize porous materials [30]. Its usage encompasses preparation of both zeolite catalysts and membrane. The growth in

the use of microwave irradiation in zeolite synthesis is due to short synthesis time and high purity and selectivity towards desired products.

Many researches have been carried out on microwave zeolitic synthesis. To start with, the synthesis of uniformly sized zeolite Y (FAU) (which is synthesized conventionally between 10-50 h) and ZSM-5 (MFI) zeolites in 10 and 30 min respectively have been reported elsewhere [31] . High Si/Al ratio (ca. 5) with low aluminum content with the absence of undesired phases was obtained.

Zeolite LTA was rapidly synthesize in a continuous flow microwave reactor [32]. Crystallization of zeolite phase under microwave irradiation is highly dependent on nucleation step and power output of microwave reactor. Different geometrical systems, spherical vessel and coiled pies showed different behavior at the same synthesis condition. Also, seeding, microwave intensity and fluid dynamic conditions were evident in product crystallinity, particle size, morphology and distribution. In addition, continuous crystallization of zeolite LTA by microwaves in the coiled pipe reactor design required an appropriate pre-seeded synthesis formulation and an exact administration of the microwave output power. LTA zeolites with the shortest synthesis time of 13 min, solution flow rate of 23 ml/min, within seeding between 0.2 and 0.1 wt% and output power between 360 W and 900 W were synthesized.

A comparative study on the synthesis of zeolite A from metakaolinite using both conventional heating and microwave irradiation heating was reported by Youssef et al [33]. The effects of reaction conditions such as NaOH molarities (1.0–5.0 M), temperatures (70 and 80 °C), synthesis time (1–8 h) as well as seeding

effect (1–4%) on the rate of formation, crystallinity and actual percentage (%) yield of zeolite A were studied. The rate of formation of zeolite A in microwave heating was about two-three time faster when compared to conventional heating with full crystallinity and higher product yield. Pure crystal phases and short crystallization time were observed for microwave irradiation technique when compared to conventional heating. Seeding using microwave irradiation technique increased the crystallization and yield of zeolite A formed as well as decreasing zeolite synthesis time.

Furthermore, Sathupunya et al reported zeolite Na-A (LTA) synthesized from alumatrane and silatrane by sol-gel microwave technique [34]. At fixed SiO_2/Al_2O_3 of 1:1 and at microwave heating of 110^oC, increasing the Na_2O (from $3Na_2O$:1 SiO_2 to $9Na_2O$:1 SiO_2) by the addition of NaOH reduces the synthesis time from 160 min to 5 min. Also, the increase in Na_2O concentration induced the formation of small crystals, whereas, low concentration of Na_2O produces large crystals. In addition, water content used during synthesis affected crystal size with reduction in molar concentration of water giving rise to smaller crystals and unequal larger crystals when concentration of water is increased. The moisture adsorption capabilities of synthesized zeolite Na-A were better when compared to commercial counterparts.

zeolite beta (BEA) was also studied in fluoride medium under microwave irradiation [35]. Zeolite beta was successfully synthesized at 150^oC within 4 h under microwave irradiation (which takes about 60 h in conventional heating). The addition of seed did not accelerate synthesis time, whereas addition of

fluoride into synthesis led to rapid crystallization. Furthermore, the addition of fluoride media accelerated nucleation rate resulting in reduced particle size.

Modernite (MOR) zeolite crystals were synthesized via microwave irradiation technique and conventional heating [36] . In the comparative study, microwave heating reduced synthesis time as well as improving phase purity and surface area when compared to conventional heating. Pure MOR crystals were synthesized within 6 h at 190^{o}C via microwave irradiation, with conventional heating producing phase impurities at the same temperature even after 72 h.

silicate-1 seeds were also synthesized by both microwave and conventional heating [37] . Chemical composition of solution gel, solution aging time at room temperature and hydrothermal synthesis condition as it affects produced seeds were investigated. The concentration of tetra propyl ammonium hydroxide (TPAOH) used as the templating agent has a dictating effect on product yield, size and aggregation. Microwave heating drastically reduced synthesis time of zeolites when compared to conventional heating. Also, increased solution aging time generally gave reduced crystal sizes. However, in order to get desired small sized silicate-1 crystals over prolonged aging time was not required when applying microwave irradiation technique.

2.5. Cracking of Hydrocarbons

The cracking of hydrocarbons have been known to occur with or without catalyst referred to as catalytic cracking or thermal cracking (in the absence of catalyst at extreme temperatures) respectively. Thermal cracking of paraffins such as n-

hexane usually starts at temperatures above 600^{o}C [38], while catalytic cracking of n-octane could be carried out at temperatures as low as 300^{o}C [39]. Above 600^{o}C, catalytic cracking carried out will be accompanied by thermal cracking. Table 2.3 below shows comparison between catalytic and thermal cracking.

2.3 : Comparison between catalytic and thermal cracking of n-hexane.

Catalytic cracking	Thermal cracking	Reference
Carbenium and Haag Dessau ion mechanism	Free radical mechanism	[40]
Ethylene and propylene yield varies with catalyst properties	Ethylene yield is always higher than propylene	[9]
Occurs at low temperatures say 400^{o}C , thus consumes less energy	Occurs at extreme temperature say 800^{o}C, thus requires more energy.	[41]

2.5.1. Mechanism of Thermal cracking.

The established mechanism for thermal cracking is free radical chain reaction. Some of the proposed mechanisms for this are the Rice-Herzfeld (R-H)[42] and the Rice-Kossiakoff (R-K)[43] mechanisms. The stages in radical chain reaction mechanism can be classified into initiation, propagation and termination. The difference between R-H and the R-K mechanisms is the decomposition and isomerization rates. The R-K mechanism holds that after the formation of radicals, isomerization of radicals comes before the decomposition of molecules into alkyl radicals. On the other hand, decomposition rate is faster than isomerization rate in the R-H mechanism at lower temperature conditions [41].

2.5.2. Mechanism of catalytic cracking of alkanes (zeolites).

For the description of catalytic cracking in zeolites, the understanding of acid sites is of great importance. Zeolites have two acid sites, Brønsted and the Lewis acid sites. Brønsted acids are proton donors, in a similar sense this definition holds for the Brønsted acid sites found in zeolites. Similarly, Lewis acids are electron acceptors. It worthy to note that for a range of zeolite catalyzed reactions, the concentration of Brønsted acid sites has a linear relation to the activity of the catalyst [38].

There are basically two main mechanisms proposed for n-alkanes cracking, the classical carbenium ion mechanism (also known bimolecular cracking mechanism) and the Haag-Dessau protolytic or monomolecular mechanism cracking.

2.5.2.1. **Classical carbenium ion mechanism**

The carbenium ion mechanism also referred to as classical cracking, β-scission or bimolecular cracking mechanism. This mechanism was attributed to the work of Greensfelder et al based on the carbenium ion chemistry [40]. This mechanism proposes the abstraction of a hydride from the reactant molecule (alkane) which results in the formation of another carbenium ion. The secondary or tertiary branched alkylcarbenium ion formed is cracked by β-scission which is the cleavage of C-C bond located β to the trivalent positively charged carbon atom [40, 44]. Furthermore, the bimolecular hydride transfer between the alkylcarbenium ion and alkane leads to a chain reaction that produces alkanes.

Cracking n- carbon atom alkanes tends to produce higher products ranging from 3 to n-3 which in turn reduces olefin yield. This mechanism is known to simultaneously involve alkylation (formation of C-C bond), β-scission (cleavage of C-C bond) and isomerization (alkyl group shift) with low probability of forming of primary alkylcarbenium ion. Thus not accounting for product distributions where ethylene, ethane and methane are formed. In addition, this mechanism did not explain the initiation of the carbenium ion.

2.5.2.2. **Haag-Dessau protolytic cracking mechanism**

Haag and Dessau in 1978 proposed a mechanism which related the chemistry of petroleum refining and Olah's hydrocarbon chemistry in superacids. The mechanism proposed that at about elevated temperatures of about 800 K [40],solid acid catalyst for such as zeolites acts as super acids that protonates a paraffin (alkane) on the strong Brønsted acid sites of zeolites to form carbonium ion [41] which in turns breakdown to produce either dihydrogen molecule (C-H cleavage) or alkanes (C-C cleavage) and carbenium ions. The carbenium ions terminate to give rise to alkenes (ethylene is achievable by this mechanism) by donating protons back to the zeolite catalyst [44]. This proposed mechanism explains the large amount of hydrogen, methane and ethane produced during the cracking process that the classical mechanism fails to explain. Furthermore, the initiation step missing in the classical cracking mechanism was explained by this mechanism.

Shape selectivity of zeolites plays an important role in determining the mechanism of catalytic cracking. As reported [40], medium pore zeolites tends to favor protolytic cracking over bimolecular hydride transfer cracking mechanism due to steric hindrance of zeolite pores. Therefore, it can be concluded that the rate of classical bimolecular cracking is directly proportional to pore size of zeolite catalyst. Hence, large pore zeolites support classical cracking over monomolecular cracking. A summarized version of the cracking mechanism of paraffins reported by Lee et al in 2011[41] is as shown in Figure 2.1 below.

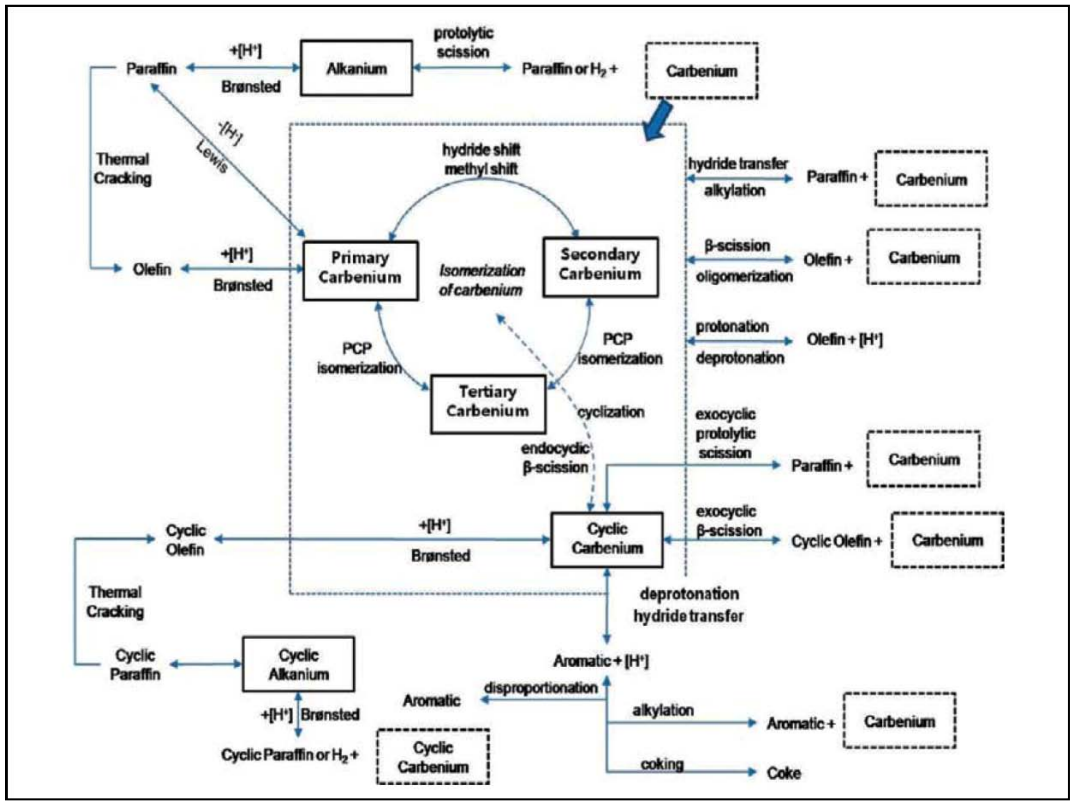

Figure 2.1 Schematic pathway of paraffins cracking (Adapted from Lee et al [41]).

2.5.3. Catalytic Cracking of Hydrocarbons over zeolites

The catalytic cracking of hydrocarbons is an important processes in the petroleum refining industries in which larger hydrocarbons are converted to lower hydrocarbons like lower alkenes and paraffins. Catalytic cracking is currently being studied as a possible replacement of steam cracking for the production of light olefins. In order to get the optimum of producing light olefins from catalytic cracking of hydrocarbons, many studies have been carried out on zeolites as potential catalytic crackers of hydrocarbons.

Xian et al (2010) [45] studied the catalytic cracking of n-dodecane over H-ZSM-5 at 400–450^{o}C in supercritical and subcritical pressures of 0.1 to 4MPa. They observed that the catalytic ability of catalyst decreases with increasing pressure. Furthermore, catalytic deactivation of catalyst also followed the same trend as catalyst activity. Also, Sicard et al (2008) [46] did a comparative study of thermal and catalytic cracking of hydrocarbons over zeolite Y (FAU) and ZSM-5 (MFI). Products obtained are functions of cracking method implemented. Pan et al [47] used modified zeolite L (LTL) in catalytic cracking of heavy oil. There achievement was improving the research octane rating (RON) of the gasoline produced. Wei et al [48] studied the catalytic cracking of naphtha at 650^{o}C over ZSM-5 modified with metals like La, Mg, Fe, Cu and P. BTX were favored products when Fe, Cu and La are used as metal loading and light olefins when Mg and P were used. Furthermore, in N_2 stream cracking using ZSM-5 modified with La about 50% of naphtha feed were converted to BTX. While in steam cracking using P and La modified ZSM-5, light olefins were readily obtained and catalyst

shows stability during reaction. Morales-Pacheco et al [49] applied nano-sized FAU(Y) and MFI(ZSM-5) zeolites with excellent surface areas and excellent thermal stability in the catalytic cracking of 1,3,5-triisopropylbenzene (1,3,5-TIPBz) in a riser simulator at 350^{o}C. Catalyst particle size plays a significant role in the conversion of reactant with smaller catalyst particles showing higher conversion compared to larger catalyst pellets.

2.6. Catalytic Cracking of n-hexane (A model reaction)

The cracking of n-hexane is an important process to produce of light olefins such as ethylene and propylene which are important chemicals in petrochemical industries. Various catalysts have been employed in this catalytic process. However, our focus is on zeolites, mainly the aluminosilicates and molecular sieves.

Many researchers put great effort in improving the amount of light olefins derived from the cracking of n-hexane. Mochizuki et al [9] reported the effect of nano-sized MFI zeolites on catalyst stability and selectivity to propylene. Three different sizes of ZSM-5 zeolites (small, medium and large) were used in the cracking of n-hexane in a tubular flow microreactor over temperature range of 723-923 K. Reactant conversion for all zeolite samples increased with elevation in temperature. Also, smaller crystal size gave higher selectivity to propylene and butylenes, while the larger crystal size was more selective to ethylene and BTX. The low selectivity to BTX in small crystals is due to steric hindrance. Furthermore, the selectivity towards ethylene and BTX increased with increasing

temperature. Rate of deactivation of catalyst was reported as a function of catalyst size, with small crystals showing higher resistivity to deactivation. Deactivation is slower in small crystals because diffusion length is shorter compared to larger crystals.

Rownahgi et al [50] studied the selective cracking of n-hexane to produce light olefins over ZSM-5 concentrating on the effect of crystal size and acid sites on nano and micron size zeolites. They reported that nano-sized zeolites of about 100nm displayed high resistivity towards deactivation and excellent selectivity of about 83% to light olefins. While in the case of the micro-sized ZSM-5 of about 2 μm selectivity towards higher hydrocarbons and resistance to coke formation was low. Their explanation to these observations was that nano-sized ZSM-5 has larger external surface area which enhances reaction in catalyst pore compared to micron-sized zeolite. They finally concluded that reducing catalyst size and reducing external surface acid sites on catalyst gives a more stable and highly selective and active catalyst for light olefins production.

2.7. MTT Zeolites as a catalyst for cracking

MTT zeolite is a one dimensional zeolite highly applied in isomerization reactions [6, 25, 51]. However, it has also shown a great potential in other reactions. Owing to its shape selective properties, its ability to cracking high molecular hydrocarbons to produce highly needed olefins could be explored. A few investigation of the catalytic cracking ability of ZSM-23 have been reported. To start with, Wang et al studied the cracking C4 alkenes over ZSM-23 [27]. Mixed

C4 alkenes were cracked over ZSM-23 with different Si/Al ratio. The number of Brønsted acid sites on synthesized catalyst increases with decreasing Si/Al ratio. Also, increment in catalytic conversion of reactants and selectivity towards desired products (olefins) follows the same trend of decreasing Si/Al ratio with the ZSM-23 having the lowest Si/Al ratio exhibiting highest activity. Furthermore, Ji et al also investigated the cracking ability of ZSM-23 over C4 alkanes [28]. Si/Al ratio plays a significant role in the activity of the catalyst. It was observed that the lower the silica to alumina ratio, the higher the catalytic conversion and selectivity towards olefins.

In this study, several strategies to improve ZSM-23 properties and its application to selective cracking of n-alkanes will be reported.

2.8. Taguchi design of experimental

In order to find the optimum properties of zeolites ZSM-23 in experimental analysis, various experimental optimization techniques such as factorial experimental method, Taguchi methods and many more have been employed. The Taguchi design of experiment developed by Taguchi Genichi is an experimental design in which minimum orthogonal arrays (OA) and analysis of variance (ANOVA) are implemented to study the effect of experimental variables on a given process. The Taguchi method is a design of experiment (DOE) that is used to obtain the contribution of given process or experimental parameters (factors) over a specified area of interest (levels) [52]. The Taguchi method optimizes a

process by the signal to noise ratio (S/N) ratio using three methods namely; the larger the better, the smaller the better and the nominal [53].

2.8.1. Taguchi orthogonal array

Taguchi orthogonal arrays (OA) are subsets of full factorial experimental method which are arranged such that parameters appear the same number of time without two experiments being similar. The OA originated from Tippett in 1934 after which tabulated simpleton forms were by Taguchi [54]. The advantage of the Taguchi OA over normal full factorial design is that it studies a large number of variables with minimal amount of experiments. The Taguchi OAs are attributed with symbol L and a number with the least being 4. The numbers represents the number of experiments and are derived by carefully arranging process parameters to appear at the same number of time.

2.8.2. Signal to Noise Ratio (S/N)

In the Taguchi method, the signal is the required or desired value (mean) of the output characteristic, while the noise is the measured output of undesired characteristics (standard deviation, SD) [53]. Thus, the ratio of the mean to the standard deviation defines the signal to noise ratio. In Taguchi method, experimental conditions with the maximum S/N ratio are considered optimal operating conditions.

2.8.3. The larger the better

When the maximum value of characteristic output is required in an experiment, the larger the better method is used in calculating the S/N ratio. The larger to better S/N ratio was reported elsewhere [53] to be calculated according to equation (2.1) :

$$\frac{S}{N} = -10 \log\left[\frac{1}{N_i}\left(\sum_{u=1}^{N_i}\frac{1}{y_u^2}\right)\right] \ldots\ldots\ldots 2.1$$

Where, i is the experiment number, N is the number of trials for i^{th} experiment, u is number of trials and y is the performance characteristics.

2.8.4. The smaller the better

When the desired value of characteristic output required in an experiment is the smallest possible value, the smaller the better method is used in calculating the S/N ratio. The formula used in calculating the S/N ratio is according to equation (2.2):

$$\frac{S}{N} = -10 \log\left(\sum_{u=1}^{N_i}\frac{y_u^2}{N_i}\right) \ldots\ldots\ldots 2.2$$

Where n is the number of tests and y_i are the comparison variables in the i^{th} experiment.

2.8.5. Nominal is the best

When the desired value of characteristic output required in an experiment is a given value, then nominal is the best is used to calculate the S/N ratio. The formula is as thus:

$$\frac{S}{N} = 10 \log \left(\frac{\bar{y}_i^2}{\sigma_i^2}\right) \ldots\ldots\ldots\ldots\ldots 2.3$$

$$\bar{y}_i = \frac{1}{N_i} \sum_{u=1}^{N_i} y_{i,u} \ldots\ldots\ldots\ldots\ldots 2.4$$

$$\sigma_i^2 = \frac{1}{N_i - 1} \sum_{u=1}^{N_i} (y_{i,u} - \bar{y}_i) \ldots\ldots 2.5$$

Where y bar is the mean and σ^2 is the standard deviation

2.9. Pareto Analysis of Variance

Pareto Analysis of variance (ANOVA) is a form of ANOVA that implements Pareto principles. It got its origin from the Pareto principle developed by the Italian economist Vilfredo Pareto in 1906. Pareto analysis is founded on the idea that 80% of a project's benefit or problem is as a result of 20% input work or causes. The Pareto principle is also known as 80/20 rule. The Pareto analysis helps in decision making by ranking causes or inputs in a line and bar plot known as Pareto plot. The Pareto ANOVA is an easy to use ANOVA since it requires no ANOVA table and consequently no F-test is required [55]. F-test is used to compare the variances of two samples to test the hypothesis that the samples are drawn from populations with different variances. The F test is calculated based on the ratio of the variances of the two samples.

CHAPTER 3

EXPERIMENTAL APPARATUS AND PROCEDURE

A summary of the experimental procedure are presented in Figure 3.1 and 3. 2.

3.1. Synthesis of MTT Zeolite

Rapid synthesis of MTT zeolites has been carried out by microwave reactor. Modification of the crystal aspect ratio (crystal length per diameter) of the rod-shape crystal of ZSM-23 will significantly reduce mass-transfer limitation problems. The effect of two important synthesis parameters, surfactant concentration and aging time were also investigated.

3.1.1. Synthesis of MTT zeolite under microwave irradiation

Synthesis was performed with colloidal silica (40 wt. %), aluminum sulfate ($Al_2(SO_4)_3$. 18 H_2O), isopropyl amine (IPA), sodium hydroxide (NaOH), polyoxyethylene 20 stearyl ether (Brij-78) and de-ionized water (H_2O).

The molar ratio of the synthesis solution was: 1 SiO_2: 0.006 Al_2O_3: 0.125 NaOH: 1.68 isopropyl amine: x Brij-78:44.52 H_2O, where x = 0, 0.04 and 0.07.

A typical solution gel was prepared by dissolving 0.31g of NaOH in 43.96g of de-ionized water, thereafter adding 0.25 g of $Al_2(SO_4)_3$.18 H_2O to form aluminate solution. After vigorous stirring for 10 min, required amount of Brij-78 surfactant was added and the temperature of solution gel was raised to 50^oC. Thereafter,

6.17 g IPA was added in a drop wise fashion to form a clear solution. Finally, 9.31 g colloidal silica (40%) was added and the mixture was stirred vigorously. Before transferring solution gel to a Teflon reactor, mixture was stirred for a specific aging time.

Solution gel prepared was heated at 453 K (180^{o}C) in a microwave reactor (MicroSYNTH, Milestone, and 400 W) for 12 h under constant stirring speed of 300 rpm. The as-synthesized zeolites were centrifuged and washed then dried at 393 K (120^{o}C) for 12 h. The OSDA was removed by calcination at 823 K (550^{o}C) for 12 h under a flow of air with the heating rate of 1 K/min. The calcined zeolites (Na-ZSM-23) were ion-exchanged and calcined again to obtain H-ZSM-23.

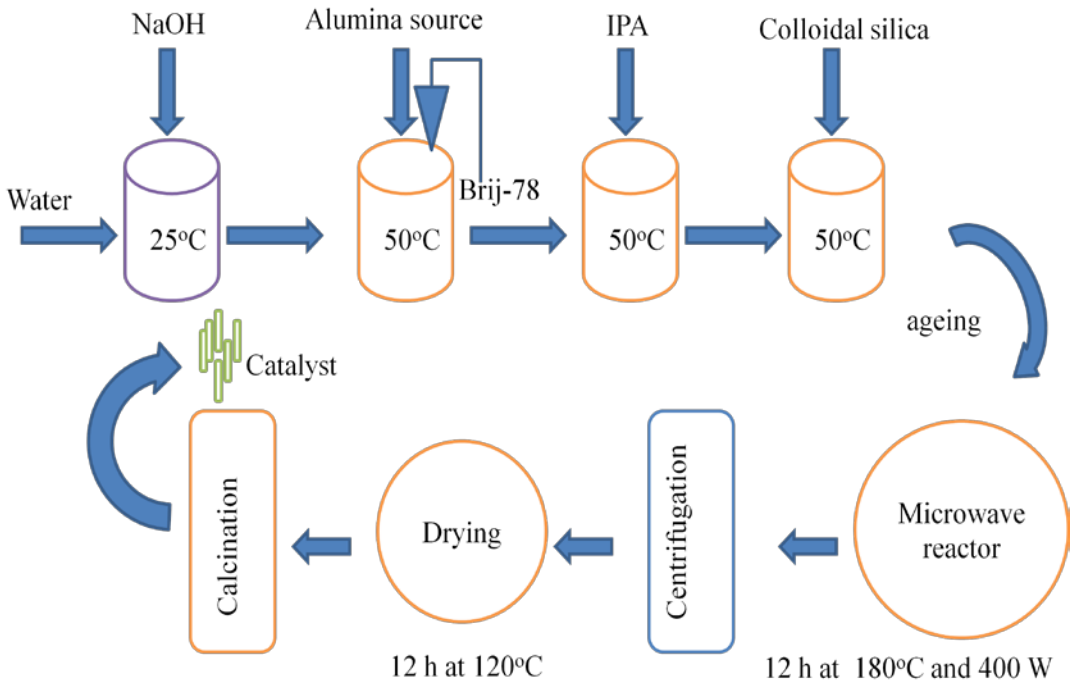

Figure 3.1 Experimental procedures for sample synthesis

3.1.2. Ion exchange under microwave irradiation

The protonated ZSM-23 (H-ZSM-23) samples were obtained by ion-exchange under microwave irradiation (250 W). Each 1 g of calcined Na-ZSM-23 was treated with 20 mL of 2 M NH_4NO_3 according to the two steps:

(i) Sample was heated from room temperature to 85^oC with ramping rate of 30^oC/min, and then dwelled at 85^oC for 10 min followed by cooling a step, and then catalyst was separated from main solution by centrifugation at 4000 rpm.

(ii) Replenishing NH_4NO_3 solution in mixture, then repeating step (i). Then, the NH_4-ZSM-23 zeolites were washed with 2-propanol. The NH_4-ZSM-23 was calcined at 550^oC for 12 h to get the proton form.

3.1.3. Desilication and mild dealumination to obtain protonated H-ZSM-23 samples

The H-ZSM-23 (3330 mg) was treated in 10 mL of 0.2 M of NaOH [56, 57] under microwave irradiation. Temperature was increased from room temperature, ramped in 2 min to reach 85^oC, and then dwelled at 85^oC for 5 min. Afterwards, sample was cooled down to room temperature by natural convection and washed several times to reduce the pH to 7.

Drying and calcinations were performed correspondingly at 140^oC for 5 h and 550^oC for 12 h. The same procedure was repeated with dwelling time of 10 min. Samples were then mildly dealuminated by microwave irradiate in 0.3 M HNO_3 for 10min at 80^oC. Thereafter, samples were washed, dried and calcined at 550^oC.

Finally, the ion exchange step was repeated to get the protonated form (H-ZSM-23).

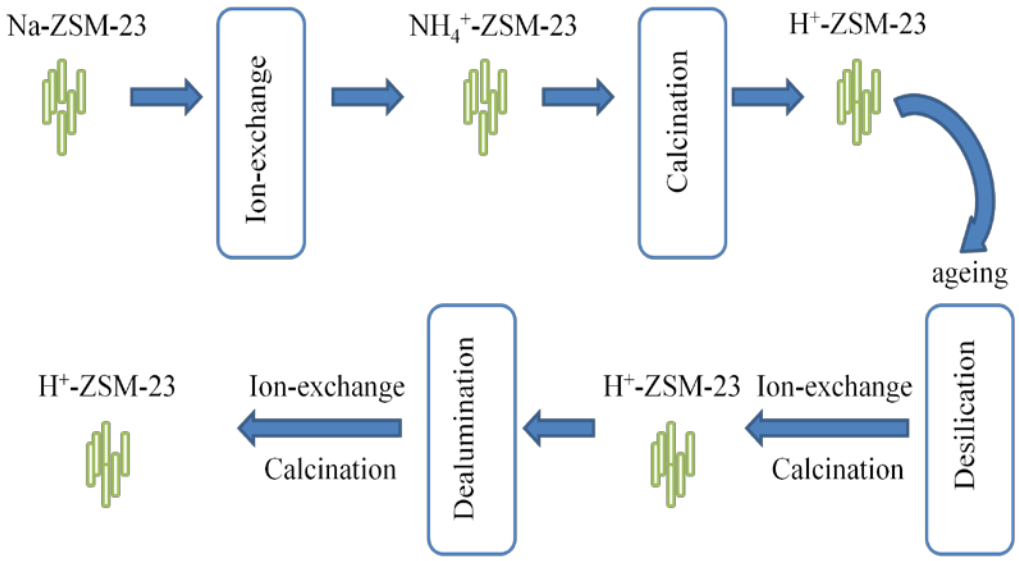

Figure 3.2 Synthesis of desilicated and dealuminated ZSM-23

3.2. Orthogonal Experimental Method

In order to optimize the role of synthesis parameters on MTT zeolite synthesis, Taguchi orthogonal experimental method was implemented. The L9 orthogonal array was used with two parameters and three levels for each parameter (see Table 3.1). In total 9 experiments were carried out to investigate the effect of two main synthesis parameters (surfactant concentration and aging time) on the synthesis of MTT type zeolite as shown in Table 3.2. Samples were designated as S-x-y, where 'x' is the mole ratio of Brij-78 surfactant to the mole of silica (Brij-

78/SiO2 ratio) multiplied by 100 and 'y' is the aging time. For example, S-4-5 is the sample synthesized using Brij-78/SiO_2 ratio of 0.04 at an aging time of 5 h.

Table 3.1 Parameters and levels of L9 orthogonal experimental method

Factors	**Level 1**	**Level 2**	**Level 3**
Brij-78/SiO_2 ratio (mol/mol)	0	0.04	0.07
Aging time (h)	5	24	48

Table 3.2 The L9 orthogonal experimental method with two parameters and three levels.

Sample experiment	Brij-78/SiO_2 ratio (mol/mol)	Aging time (h)
S-0-5	0	5
S-0-24	0	24
S-0-48	0	48
S-4-5	0.04	5
S-4-24	0.04	24
S-4-48	0.04	48
S-7-5	0.07	5
S-7-24	0.07	24
S-7-48	0.07	48

3.3. Catalytic testing and product analysis

The catalytic activities of ZSM-23 zeolites were tested in catalytic cracking of light naphtha by using n-hexane as model compound. Catalytic cracking of n-hexane was carried out at 923 K (650 ^{o}C) over H-ZSM-23 in a pack bed reactor (ID: 9.8 mm and OD 12.7 mm) loaded with 300 micron zeolite pellet without

binder. The W/F was 0.125 h, where W is amount of catalyst [g] and F is feed rate [g h^{-1}]. The n-hexane was used as a model compound with volumetric feed rate of 1.8 ml/h. Controllable range of the liquid pump (kd scientific) was 0.1- 50 ml/h. The nitrogen of 20 ml/min flow rate was used as a carrier gas.

The reaction product was analyzed by two connected online gas chromatograph (GC, Shimadzu GC-2014). The first GC has FID and a packed column (SP-1700) and TCD (column is Porapak). The second GC has FID (column is gaskuropak). Figure 3.3 shows a typical packed bet reactor set up for n-hexane cracking.

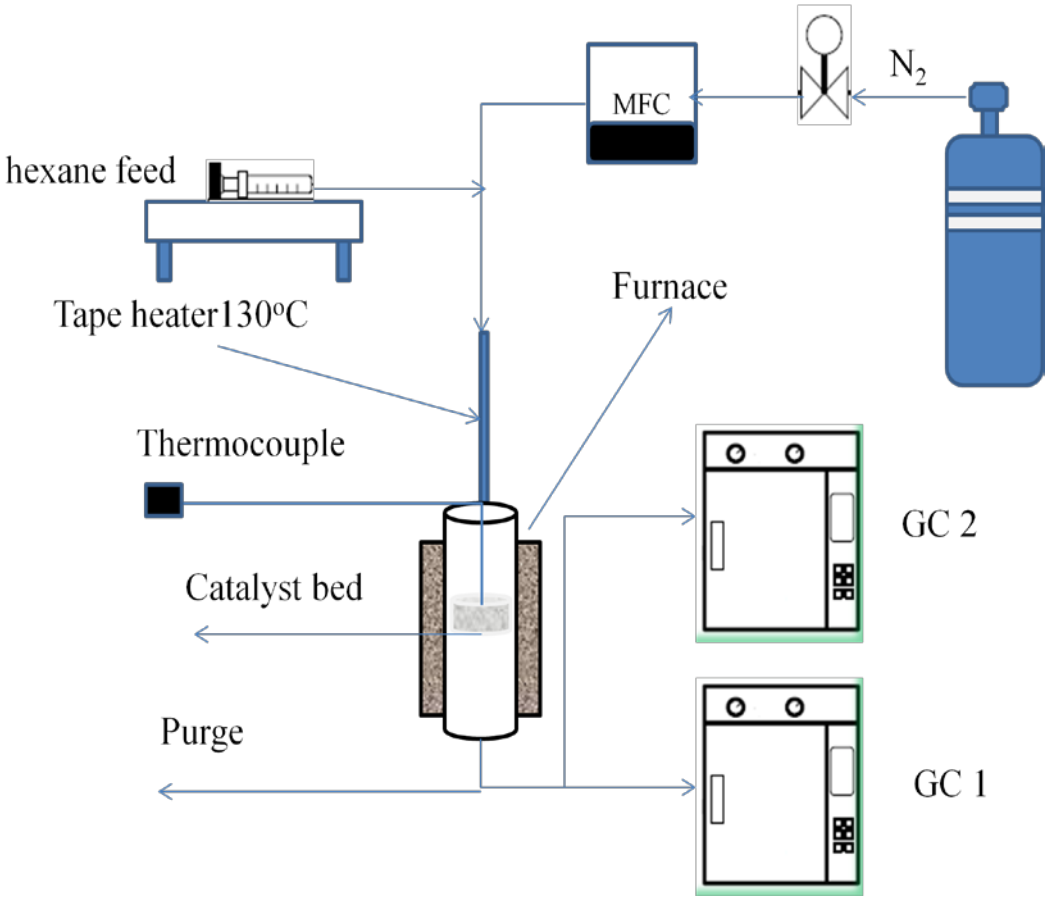

Figure 3.3: Packed bed reactor set up for n-hexane cracking.

CHAPTER 4

RESULT AND DISCUSSION

4.1. Characterization of ZSM-23 catalyst

X-ray diffraction analysis of as-synthesized samples showed that all samples were pure MTT-zeolite phase (Figure 4.1) with the exception of S-0-5 which contains traces of ZSM-5 zeolite. Although it was not observed in XRD patterns, the presence of ZSM-5 as an impurity phase was clear from FESEM image as shown in Figure 4.2 made it more evident. The appearance of trace amount of ZSM-5 as a competing phase is possible when using IPA as structural directing agent as reported by Liu et al in their studies [26]. FESEM images in Figure 4.3 further show that samples morphology was rod-like. The bundles of needle observed in sample synthesized by conventional heating were absent. The absence of these bundles might be as a result of agitation in the microwave reactor during synthesis and slower agglomeration rate. It was reported elsewhere [8] that conventional synthesis produce ZSM-23 zeolites of about 10 μm in length. However, in our studies we found that smaller ZSM-23 zeolites can be produced in the sub-micron region, as will be elaborated later. The reason is that microwave heating enhances the crystallization rate and simultaneously shortens synthesis time compared to the rate in hydrothermal heating. Therefore, due to the short synthesis time spent by samples under microwave irradiation, overgrowth of zeolite crystals was avoided.

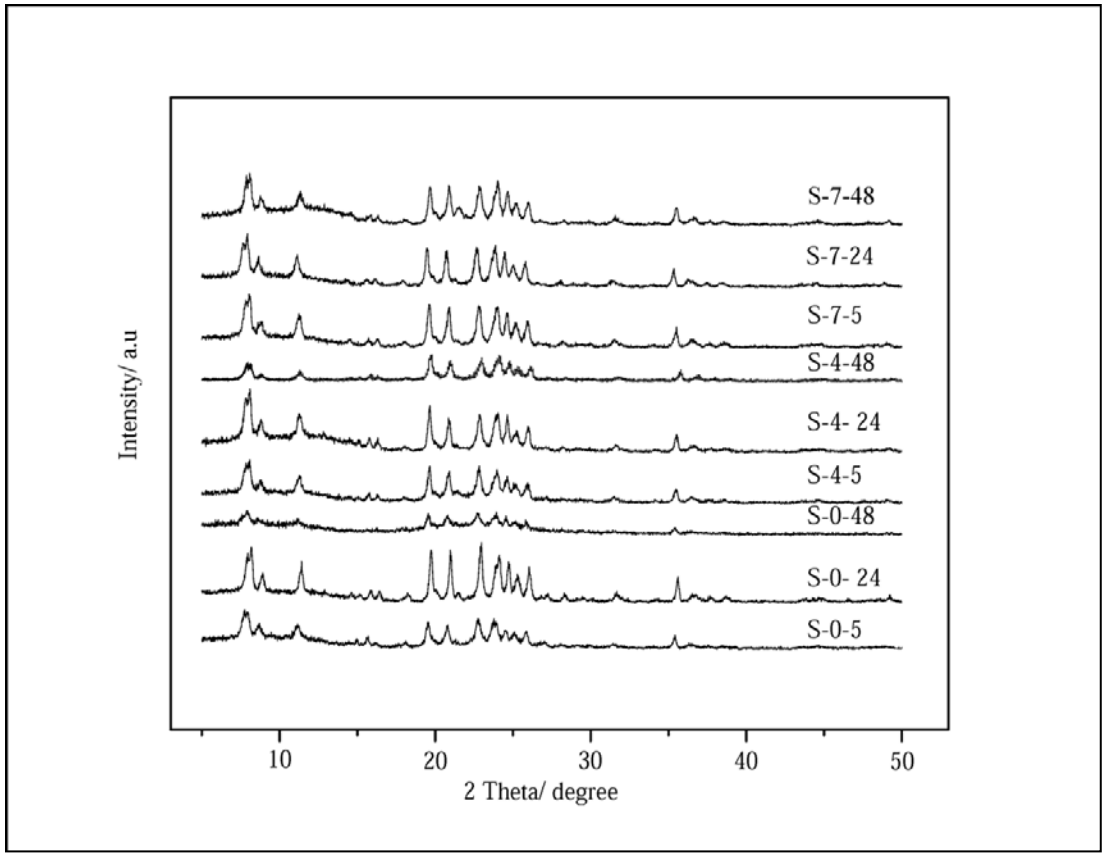

Figure 4.1 XRD pattern of as-synthesized samples.

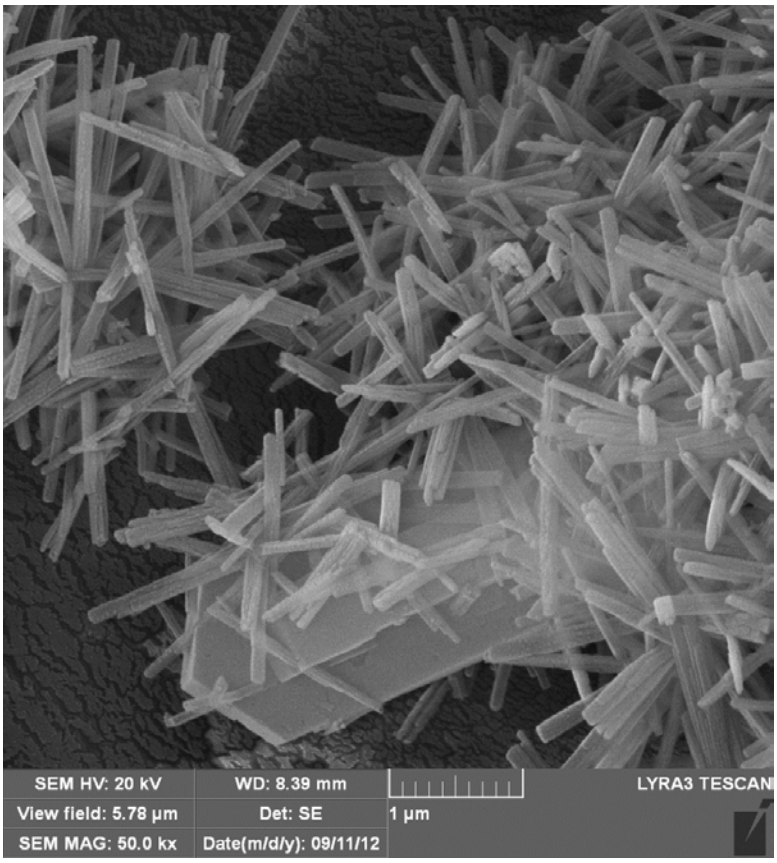

Figure 4.2 FESEM image of S-0- 5 showing trace of ZSM-5 phase.

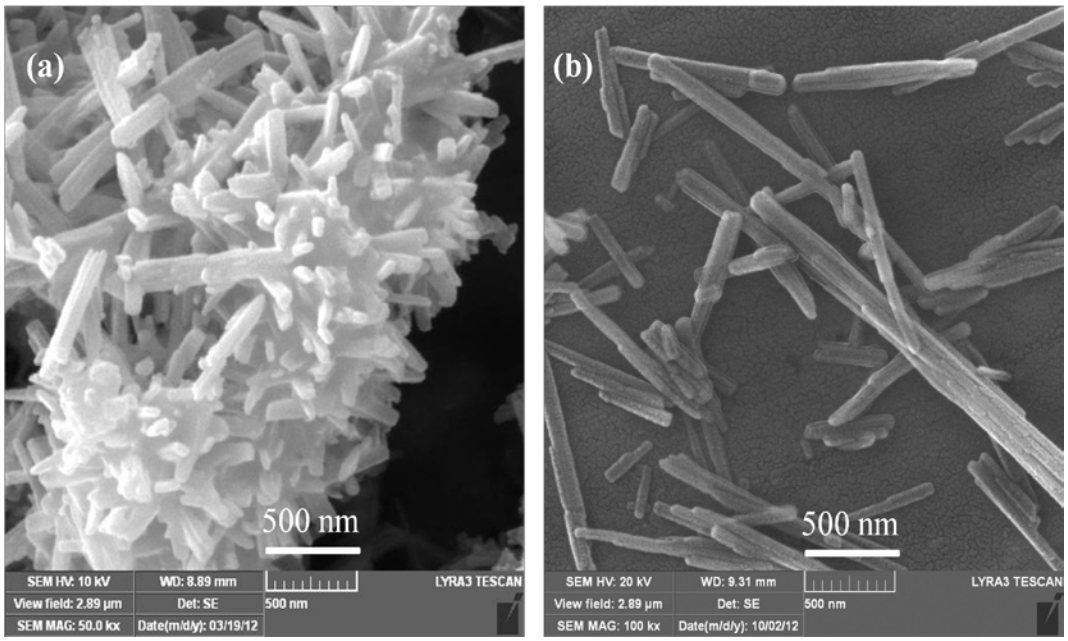

Figure 4.3 FESEM image of samples synthesized at 180^{o}C for 48 h with different Brij-78/SiO_2 ratio (a) S-0-48 and (b) S-4-48 .

4.2. NMR Analysis

The ^{27}Al and ^{29}Si MAS NMR spectra of zeolite sample S-7-48 is presented in Figure 4.4.We observed Al seated in the tetrahedral position of the zeolite framework. Also, the Si specie of sample was positioned in the tetrahedral position of the zeolite framework. The Si/Al ratios by EDX of as-synthesized samples are as shown in Table 4.1. We observed that the incorporation of Si and Al into the zeolite framework is dependent on aging time and Brij-78/SiO_2 used during synthesis.

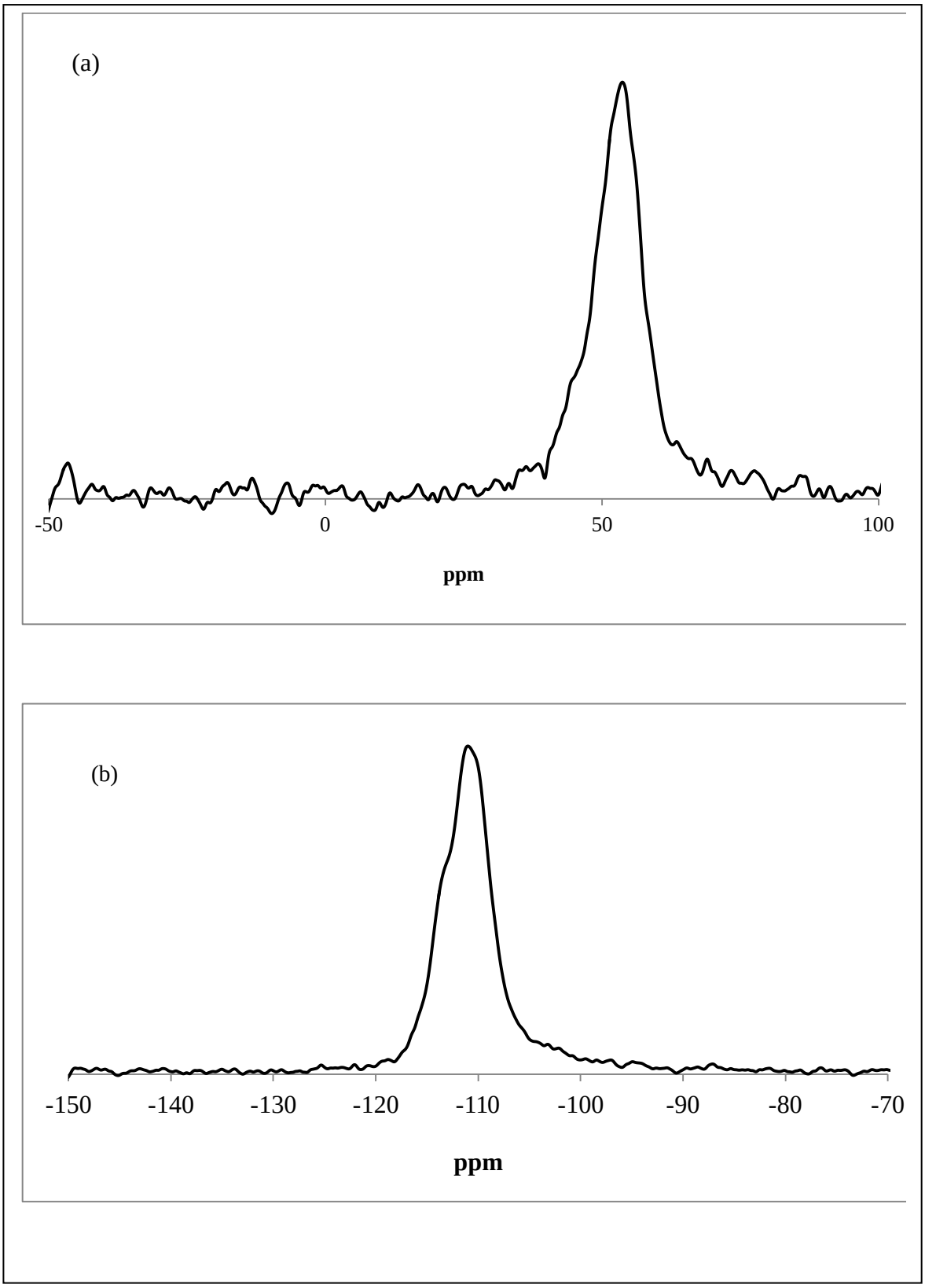

Figure 4.4 Solid-state ^{27}Al and ^{29}Si MAS NMR spectra, of calcined MTT zeolite sample (S-7-48).

Table 4.1 Si/Al ratio of samples measured by EDX.

Samples	Brij-78/SiO_2 ratio	Aging time (h)	Si/Al ratio
S-0-5	0	5	54
S-0-24	0	24	59
S-0-48	0	48	46
S-4-5	0.04	5	87
S-4-24	0.04	24	59
S-4-48	0.04	48	59
S-7-5	0.07	5	52
S-7-24	0.07	24	75
S-7-48	0.07	48	56

With the confirmation of the phase present as MTT-zeolite, what is next in line is to investigate the effects and contributions of synthesis parameters, surfactant concentration and aging time on as-synthesized samples. As mentioned previously, Taguchi design of the experiment was applied where the signal to noise ratio (S/N ratio) of characteristic properties (mean crystal length and BET surface area) plays a significant role in assessing the effects of process design factors. Since we intend to minimize the mean crystal length and to maximize catalyst the BET surface area, we used two techniques. The larger the better (see equation 2.1) was used to maximizing the BET surface area and the smaller the better was used for crystal length (see equation 2.2) since minimization is required. However, in both cases S/N ratio is always maximized.

4.3 Effect of synthesis parameter on mean crystal length

4.3.1. *Effect of aging time at fixed Brij-78/SiO_2 ratio on mean crystal length*

Aging of solution gel before crystallization is a well-known process used to suppress unwanted impurity phases aside the desired zeolite phase [58]. Aging of synthesis mixture favors nucleation over crystal growth which in turn results in shorter crystal sizes. Investigating the effect the effect of aging time and Brij-78 surfactant will give us a better insight on how these parameters affect the crystal length [59].

Mean crystal lengths of as-synthesized samples measured from FESEM images taken from different sections of the samples are shown in Table 4.2. In order to give a clear explanation of the effect of synthesis parameters, Brij-78/SiO_2 ratio and aging time on mean crystal length, interaction plot was constructed as shown in Figure 4.5. When Brij-78/SiO2 ratio was fixed while aging time was varied, a defined pattern of length reduction with increasing aging time was observed for all levels of Brij-78 surfactant (see Figure 4.5a). Our studies show that the rate of mean crystal length reduction is fastest when Brij-78/SiO_2 ratio was fixed at 0 (see Figure 4.5a). For instance, we observed that at level zero, the mean crystal length was in the sequence S-0-5 > S-0-24 > S-0-48. This result is expected since at the initial level when no surfactant was added, increasing synthesis aging will lead to the formation of more nuclei. Thus, nucleation rate is more dominant than the crystal growth rate, therefore crystal length becomes smaller with prolonged aging time. Furthermore, when Brij-78/SiO_2 ratio was fixed at 0.04 and 0.07 levels, decrease in mean crystal length with increasing aging time was observed.

Table 4.2 Textural properties of MTT-zeolite samples

Samples	Brij-78/SiO_2 ratio	Aging time (h)	BET surface area[a] (m^2/g)	S/N ratio BET surface area	Mean crystal length (nm)	S/N ratio mean crystal length
S-0-5	0	5	178	45.0252	667	-56.4890
S-0-24	0	24	210	46.4561	356	-51.0306
S-0-48	0	48	91	39.1353	193	-45.7053
S-4-5	0.04	5	154	43.7617	467	-53.3819
S-4-24	0.04	24	182	45.2166	407	-52.1891
S-4-48	0.04	48	205	46.2378	367	-51.2847
S-7-5	0.07	5	220	46.8440	737	-57.3484
S-7-24	0.07	24	162	44.1739	409	-52.2375
S-7-48	0.07	48	174	44.8201	322	-50.1476

[a] Measured from protonated form of samples (H-MTT-zeolite)

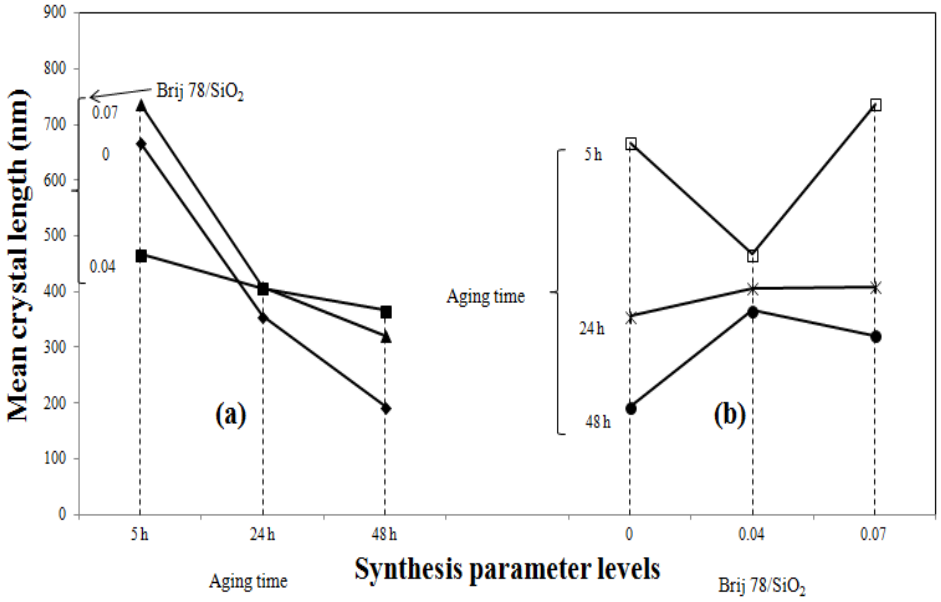

Figure 4.5 Interaction plot of synthesis parameter for mean crystal length.

4.3.2. *Effect of Brij-78/SiO_2 ratio at fixed aging time on mean particle size*

An inconsistent behavior was also observed when the aging times were fixed at different levels with variations of Brij-78/SiO_2 ratio (see Figure 4.5b). For instance, at 5 h synthesis aging time, increasing the Brij-78/SiO_2 ratio from 0 to 0.04 led to a decrease in catalyst mean crystal length. However when Brij-78/SiO_2 ratio was increased to the third level of 0.07 an increase in crystal length was observed. The length observed was greater than the initial length when the Brij-78/SiO_2 ratio was zero. A different trend was observed when the synthesis aging time was fixed at 24 h; increasing the Brij-78/SiO_2 ratio generally gives rise to an increase in crystal length.

From the interaction plot study, we observed that there was no clear trend for the effect of Brij-78/SiO_2 ratio except when aging time was fixed at 24 h. This might be as a result of type of micelles formed fluctuating with change increasing Brij-78/SiO_2 ratio. However, the average effect observed when Brij-78/SiO2 ratio is increased is a corresponding increment in mean crystal length as will be explained later using Taguchi analysis. This is also similar to report by Tago et al [ ] where they observed that increasing the concentration of nonionic surfactant above an optimal point resulted in an increase in mean crystal length of zeolites (MOR). The addition of the optimum amount of surfactant with co-solvent induces both nucleation and crystallization resulting in the formation of monodispersed MOR nanocrystals. However, further increment in surfactant concentration leads to over stabilization of precursor which brings about high

viscosity of solution gel. This high viscosity thus leads to decrease in nucleation rate and encourages formation of longer crystals [60] .

The effect of synthesis parameters on mean crystal length as discussed above is summarized in the following points:

I. At fixed Brij-78/SiO_2 ratio and variation of aging time :
   - Increasing aging time led to decreasing mean crystal length.

II. At fixed aging time and variation of Brij-78/SiO_2 ratio :
   - There was also no consistent trend except when aging time was fixed at 24 h. At this point, increasing Brij-78/SiO_2 ratio led to increasing mean crystal length.

III. Minimum mean crystal length of 193 nm was observed at 0 Brij-78/SiO_2 ratio and 48 h (sample S-0-48).

4.4 Effect of synthesis parameter on BET surface area

4.4.1 *Effect of aging time at fixed Brij-78/SiO_2 ratio on BET surface area*

Table 4.2 also shows the BET surface area of as-synthesized samples. The interaction plot as shown in Figure 4.6 is also valuable in explaining the effects of aging time and Brij-78/SiO_2 ratio. Brij-78/SiO_2 ratio was fixed at different levels in order to see the effect of aging on BET surface area. As shown in Figure 4.6a , when Brij surfactant was not used (Brij-78/SiO2 ratio = 0), increasing the synthesis aging time from 5 h (S-0-5) to 24 h (S-0-24) led to an increase in sample BET surface area of 178 m^2/g to 210 m^2/g. A further increase in synthesis aging

time to 48 h (S-0- 48) led to a decrease in the BET surface area to a value of 91 m^2/g. The reason for a low BET surface area recorded in sample S-0-48 might be due to pore blocking in one- dimensional zeolites. Three possibilities for pore blocking were proposed elsewhere [ ] : structural defect in main channels, presence of amorphous material and localization of cations. The localization of cation cannot be the reason for the low sorption property recorded since all samples BET surface area were measured after ion exchange. Thus the reason for the low BET surface area might either be due to partial pore mouth blocking by amorphous silica or structural defect in the relatively narrow non–intersecting channels which are common to the MTT zeolite [8]. N_2 Sorption report has shown in Appendix A further emphasizes that the low BET surface area is mainly from the micropores of sample S-0-48. We observed that sample exhibits relatively high mesoporous surface area and volume when compared to all other samples. However, micropore volume and micropore surface area are quite small (approximately 2.5 times smaller to other samples) when compared to other samples. Aging of synthesis mixture favors nucleation over crystal growth [ ], and the more nucleus formed, the more Si and Al species are required for the formation of zeolite framework. Since the SiO_2 to Al_2O_3 ratio in synthesis is high (>100), the possibility of complete consumption of Al specie is might be expected due to excessive nuclei formation. Hence, it might be that excess Si species that are not incorporated into the zeolite framework tends to form amorphous silica inside the micropore of zeolite framework.

When the Brij-78/SiO_2 ratio was increased to its second level of 0.04, a steady increment of the BET surface area of samples with increasing aging time was observed. At the final Brij-78/SiO_2 ratio of 0.07, an increase in aging time from the initial 5 h period to 24 h led to decrease in BET surface area. However when the aging time was further increased to 48 h, the BET surface area increases to ca. 170 m^2/g. As discussed earlier, the interaction between hydrophilic and hydrophobic parts of nonionic surfactant with precursor solution leads to micelles formation that affects both solution viscosity and surface tension. This in turns affects nucleation and crystal growth rate. The extent to which the precursor's solution physicochemical properties are affected is a function of surfactant concentration. When the Brij-78/SiO_2 was fixed at 0.04, there is improvement in the BET surface area with increasing aging time. This suggests that the effect of surfactant at this level of concentration induces nucleation and prevents crystal growth in such a way that crystals are shorter and BET surface area is larger. Here, we assume that the allowable Brij-78/SiO_2 ratio is the range of 0-0.04. Within this region, addition of poly oxyethene surfactant such as Brij-78 can reduce the crystal length and result in large surface area.

Figure 4.6 Interaction plot of synthesis parameter for BET surface area

4.4.2 *Effect of Brij-78/SiO2 ratio at fixed aging time on BET surface area*

Also, no clear trend was observed when aging time was fixed and Brij-78/SiO2 ratio was varied as shown in Figure 4.6 b. However, at 24 h aging time, the amount Brij-78/SiO_2 ratio is inversely proportional to BET surface area with increasing Brij-78/SiO_2 ratio resulting in a decrease in BET surface area.

All samples were prepared at a constant aging temperature of 50^{o}C; the characteristic properties of Brij-78 surfactant might vary at different points during the aging period (micelle formation and deformation, shape of micelle formed and many more). This change in characteristic properties of Brij-78 surfactant at different point can therefore affect the nucleation and crystallization rates of as-synthesized zeolites, the round effect which is expressed in the BET surface area.

In summary, addition of Brij surfactant to synthesis solution brought about improvement in BET surface area even at extended aging. Furthermore, we observed that in the absence of Brij surfactant, extended aging of solution gel for 48 h led to poor surface area of $91 m^2/g$ (S-0-48). However, the addition of Brij-78 surfactant at 0.04 and 0.07 Brij-78/SiO_2 ratios at the same extended aging time (48 h) give rise to improved surface areas of $205 m^2/g$ (S-4-48) and $174 m^2/g$ (S-7-48) respectively.

The effect of synthesis parameters on BET surface area as discussed above can be summarized into the following points:

IV. At fixed Brij-78/SiO_2 ratio and variation of aging time :
    - There was no consistent trend except when Brij-78/SiO_2 ratio was fixed at 0.04. At this point, increasing aging time led to increasing BET surface area.

V. At fixed aging time and variation of Brij-78/SiO_2 ratio :
    - There was also no consistent trend except when aging time was fixed at 24 h. At this point, increasing Brij-78/SiO_2 ratio led to decreasing BET surface area.

VI. Maximum BET surface area of $220 m^2/g$ was observed at 0.07 Brij-78/SiO_2 ratio and 5 h (sample S-7-5).

VII. The optimum sample is the sample with the highest S/N ratio when the summation of S/N ratios for mean crystal length and BET surface area is carried out (Appendix C). From our calculation, sample S-0-24 h is

optimum. This is because the simultaneously decrease in mean crystal length and increase BET surface area is maximum in this sample.

4.5 Taguchi Analysis

Taguchi design of experiments as an analysis tool is useful is telling the contribution of process parameters in a given process. The use of this tool for zeolite synthesis and modification has been reported elsewhere [54, 62]. To properly understand the effect of process parameters on a particular process the signal to noise ratio (S/N ratio) was studied. We applied *the smaller the better method* and *the larger the better method* for calculating the S/N ratio of mean crystal length and BET surface area respectively. In some cases where the Taguchi method was implemented, interaction between parameters did not really contribute in any way to the studied characteristic property. However, in this study, the interaction between the two studied process parameter is significant has evident in the overlaps in interaction plots (see Figure 4.5 and 4.6). It is noteworthy that in both cases of *the larger the better* and *the smaller the better* techniques, S/N ratio is always maximized. In *the larger the better* technique which was used for the BET surface area, highest number of the S/N ratios corresponds to the highest value of BET surface area. While in *the smaller the better* technique used for mean crystal length, the highest number of S/N ratio corresponds to the minimum value of mean crystal length.

Figure 4.7 Mean effect of synthesis parameter on BET surface area.

Taguchi analysis calculates the effect of parameters on characteristic properties (BET surface area and mean crystal length) using the mean effect of the S/N ratio of the factors (synthesis parameters). The mean effect of synthesis parameters is presented in Appendix B. Figure 4.7 shows the plot of mean signal to noise ratio of synthesis parameters on BET surface area. A, B and AxB were used to denote Brij-78/SiO_2 ratio, aging time and the interaction between Brij-78/SiO_2 ratio and aging time respectively. Whereas, numeric 1,2 and 3 stands for levels of these parameters. For example, A1 indicates Brij-78/SiO_2 ratio at level 1 (Brij-78/SiO_2 = 0). The mean effect plot indicates that the Brij-78/SiO_2 ratio leads to increasing average signal to noise ratio with increasing level of Brij-78/SiO_2 ratio. This shows that on the average, as the Brij-78/SiO_2 ratio is increased, the BET surface area is also increased. Whereas on the average, an optimum increment is observed

when aging time is increased, after which a decline in BET surface area is observed. In addition, to measure the effect of synthesis parameters on the BET surface area; Taguchi method suggests measuring the *delta value* of the mean S/N ratio of synthesis parameters. The *delta value* measures the significance of each synthesis parameter, with the parameter having the largest delta value being the most significant. For example, the delta value of the Brij-78/SiO_2 ratio is the maximum mean S/N ratio (A3) minus the minimum mean S/N ratio (A1). We see in Figure 4.8 that contribution was competitive. However, the aging time still has the most significant effect on the BET surface area of catalyst.

Figure 4.8 Taguchi delta plot of the effect synthesis parameter on BET surface area and mean crystal lengths, where A, B and AxB are Brij-78/SiO2 ratio, aging time and their interaction respectively.

In the case of mean crystal lengths of catalyst samples, mean effects of the S/N ratio of synthesis parameters were also used as explained above (see Figure 4.9). We observe that the average S/N ratio of Brij-78/SiO_2 ratio decreases with increment in level. This implies that increasing the Brij-78/SiO_2 ratio on the average leads to an increase in mean particle size. While increasing the aging time on the average leads to decreasing mean crystal length. Calculation of delta value of the mean effect plot shows that the aging time plays the most important role in minimizing mean crystal length of as a synthesized sample (see Figure 4.8).

Figure 4.9 Mean effect of synthesis parameter on mean crystal length

4.6 Pareto Analysis of variance

Another alternative statistic tool to measure the contributions of synthesis parameter is the Pareto ANOVA. It uses the *sum of squares* (SS) values measured from the S/N ratio of synthesis parameters. The contribution of synthesis parameters on the BET surface area as calculated by the Pareto ANOVA method is shown in Table 4.For Brij-78/SiO2 ratio (A) the SS was calculated as thus $(A1-A2)^2 + (A1-A3)^2 + (A2-A3)^2$. From the calculated SS values, percentage contributions of synthesis parameters were then calculated. We observed a competitive contribution of 34.06% for Brij-78/SiO_2 ratio, 42.97 % aging time and 22.96% for their interaction (see Table 4.3). This result is similar to the prediction via Taguchi method. In concession with the Taguchi method, the Pareto ANOVA's prediction of the effect of synthesis parameters on as-synthesized sample's mean crystal lengths is as shown in Table 4.4. We also observe that the aging time has the highest contribution of 83.95% on the mean crystal length. This is followed by the Brij-78/SiO2 ratio which has 8.77% and then their interaction with 7.27%.

Table 4.3 Pareto ANOVA for BET surface area.

	Factors and interaction			
Sum of factor in level	Brij-78/SiO_2 ratio (A)	Aging time (B)	Interaction (AxB)	Total
1	130.62	135.63	135.44	401.68
2	135.22	135.85	131.20	402.26
3	135.84	130.19	135.04	401.07
Total	401.67	401.67	401.67	**1205.01**
Sum of squares of differences (S)	48.81	61.58	32.90	143.29
Contribution (%)	34.06	42.97	22.96	100
Pareto diagram	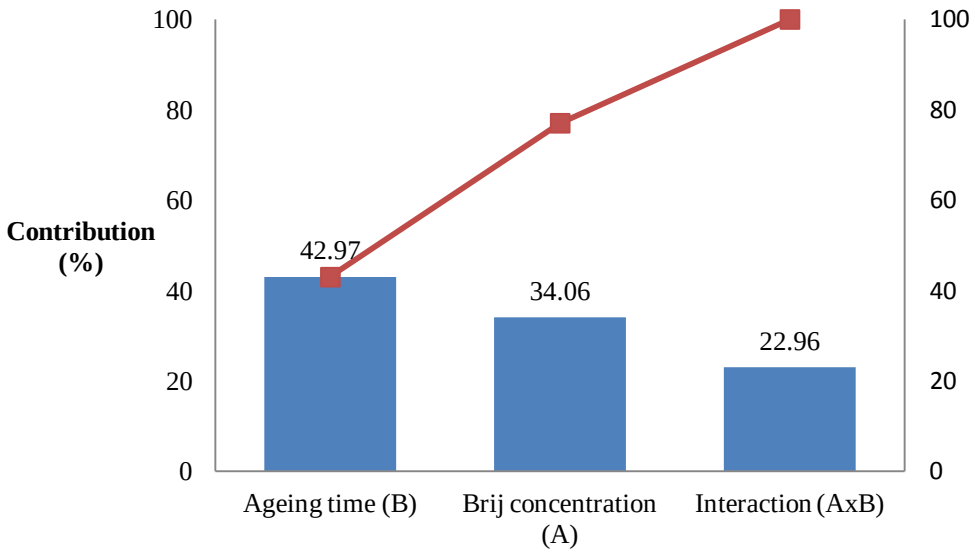			
Cumulative contribution (%)		42.97	77.03	100.00

Table 4.4 Pareto ANOVA for mean crystal length.

	Factors and Interaction			
Sum of factor in level	Brij-78/SiO2 ratio (A)	Aging time (B)	Interaction (AxB)	Total
1	-153.22	-167.22	-160.01	-480.46
2	-156.86	-155.46	-155.24	-467.56
3	-159.73	-147.14	-154.56	-461.43
Total	-469.81	-469.81	-469.81	-1409.44
Sum of squares of differences (S)	63.83	610.84	52.92	727.59
Contribution (%)	-153.22	-167.22	-160.01	-480.46
Pareto diagram	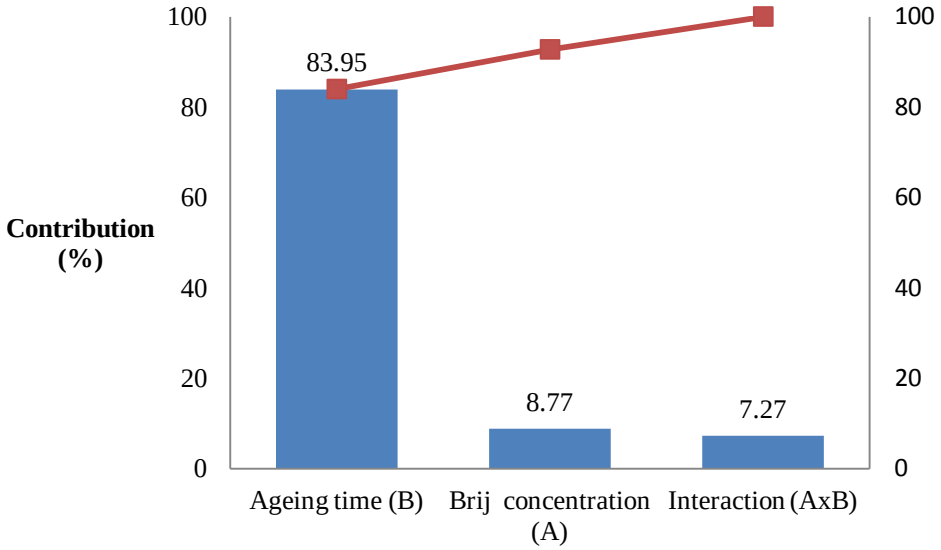			
Cumulative contribution (%)		83.95	92.72	100.00

4.7 Catalytic cracking of n-hexane over MTT-zeolite

The activities of as-synthesized MTT-zeolite samples were investigated in the cracking of n-hexane. The activities of two trials, **S-7-5** (220 m^2/g, 727 nm) and **S-7-48** (174 m^2/g, 322 nm) with mean crystal lengths were investigated. Conversion, selectivity and product yield were calculated as shown in equations 4.1, 4.2 and 4.3 respectively. Figure 4.10 and 4.11 show the conversion and selectivity of samples S-7-5 and S-7-48 respectively at 923K. Since catalytic

cracking was done at a temperature range were thermal cracking is possible, conversion due to thermal cracking needs investigation. Studying the thermal cracking of n-hexane at this condition, we observed only 15% conversion. This shows that the high conversion of approximately 80% observed initially is mainly due to catalytic cracking by as-synthesized MTT zeolite samples. Though **S-7-5** showed a slightly higher initial conversion than **S-7-48,** this is probably due to the presence of higher amount of acid sites as shown in Table 4.5. However, average conversion over time on stream was higher in **S-7-48**. This might be as a result of lower resistance to diffusion in **S-7-48** when compared to **S-7-5**. The low resistance diffusion is a function of smaller mean crystal length of **S-7-48**.

Table 4.5 NH3 TPD of MTT-zeolite samples

Catalyst	NH_3-TPD ($mmolg^{-1}$)			
	Total acidity	Low temperature L.T. (weak)	High temperature H.T. (medium- strong)	H.T/L.T.
		< 300 °C	300 - 650 °C	
S-7-5	0.277	0.128 (270)	0.149 (479)	1.16
S-7-48	0.267	0.120 (263)	0.147 (470)	1.24

Selectivity towards desired products was observed in both S-7-5 and S-7-48. In both cases, selectivity towards desired olefins was stable. Approximately, 58% selectivity was observed for both catalysts over time on stream. The selectivity

towards paraffins increases at a slow rate with increases time on stream averaging ~40% in both catalyst. In all instance selectivity towards olefins is always higher than paraffins. Furthermore, selectivity towards methane and BTX were minimal in both catalysts. The low selectivity towards BTX might be as a result of medium-sized crystals of catalyst used. Studies made by Mochizuki et al shows that large crystals favors BTX formation, where medium and small sized crystals favors olefins formation [9].

$$\boldsymbol{Conversion}\ (\%) = \frac{\boldsymbol{n-hexane\ converted}}{\boldsymbol{n-hexane\ \ injected}} \times \mathbf{100}\% \quad \ldots\ldots\ldots\ldots\ldots\ldots\ 4.1$$

$$\boldsymbol{Selectivity}\ (\%) = \frac{\boldsymbol{amount\ of\ desired\ preoduct}}{\boldsymbol{amount\ of\ total\ product}} \times \mathbf{100}\% \quad \ldots\ldots\ldots\ldots\ldots\ 4.2$$

$$\boldsymbol{Yield}\ (\%) = \frac{\boldsymbol{product\ selctivity}}{(\mathbf{100}-\boldsymbol{n-hexane\ selectiviy})} \times \mathbf{100}\% \quad \ldots\ldots\ldots\ldots\ldots\ldots 4.3$$

Figure 4.10 Plot of selectivity and conversion versus reaction time for sample S-7-5.

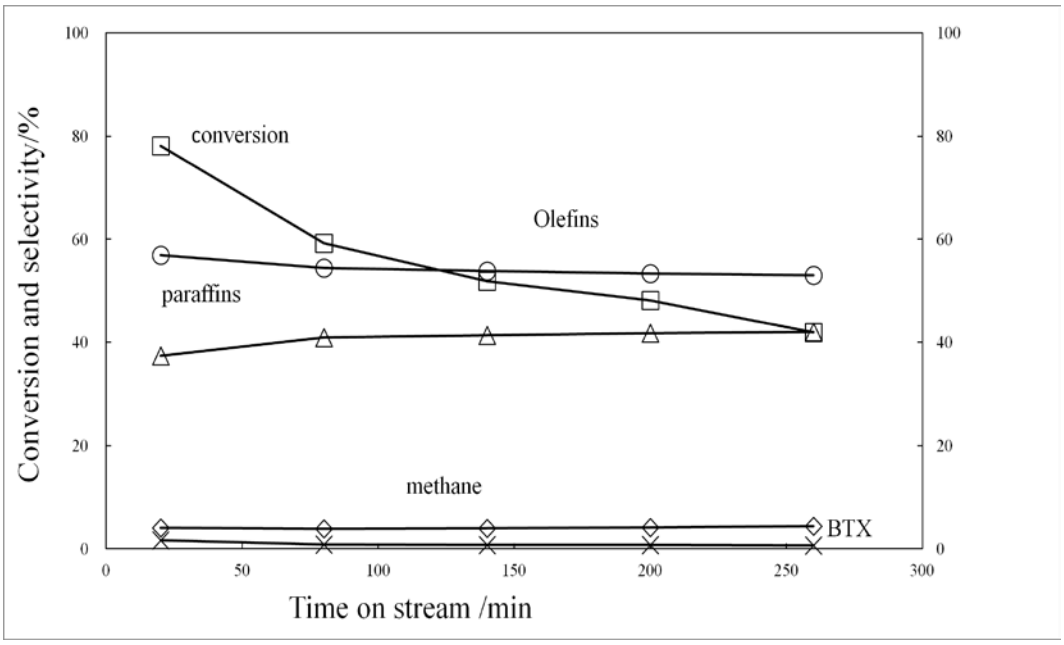

Figure 4.11 Plot of selectivity and conversion versus reaction time for sample S-7-48.

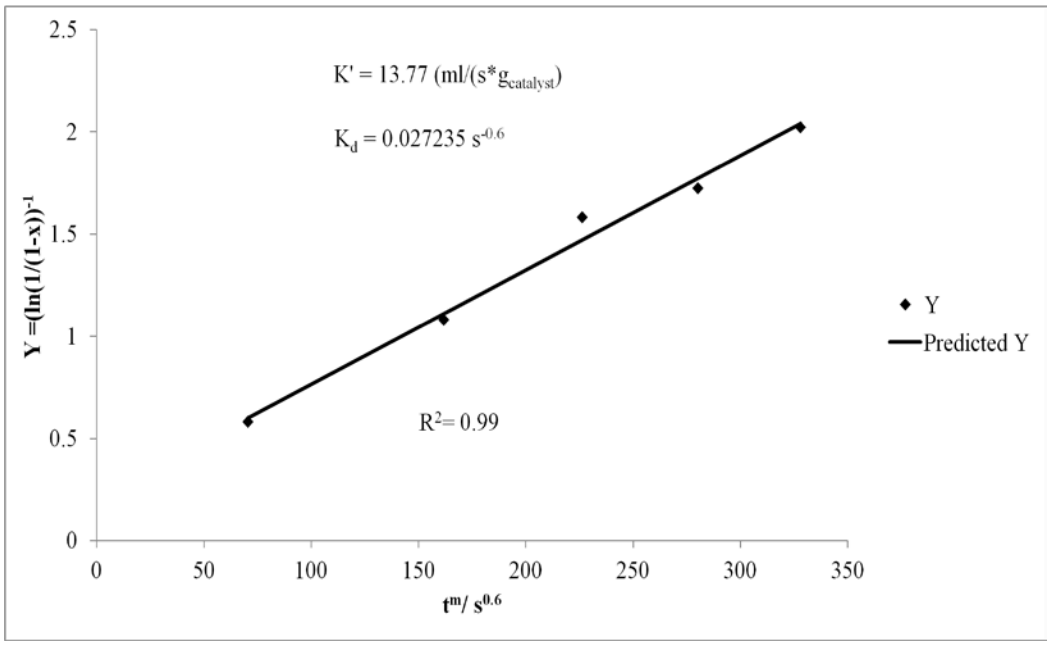

Figure 4.12 Plot of experimental and model prediction for n-hexane cracking for S-7-5

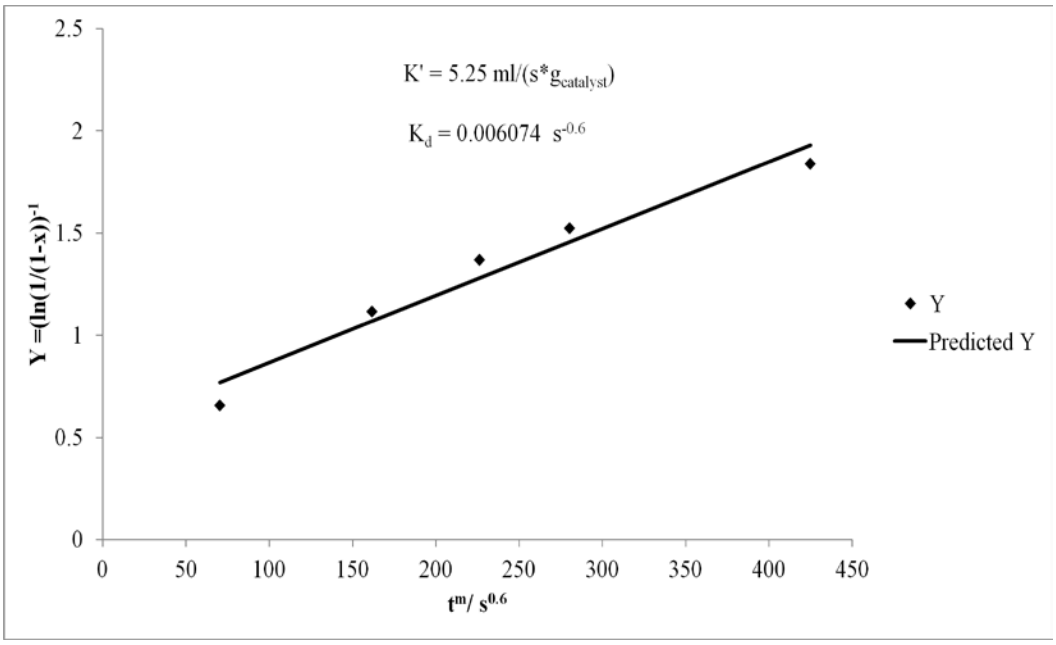

Figure 4.13 Plot of experimental and model prediction for n-hexane cracking for S-7-48

Deactivation constants calculated via modified second order deactivation rate [63] and first order kinetics of n-hexane cracking shows that deactivation constant in **S-7-5** is 0.027235 $s^{-0.6}$ and that in **S-7-48** is 0.006074 $s^{-0.6}$ (see equation 4.1 and Figure 4.12 and 4.13). It means that deactivation in **S-7-48** is slower than that in **S-7-5**. This is because the mean crystal length (crystal length) in **S-7-48** is smaller than that in **S-0.07-5**. This agrees with reports elsewhere [, 64] that reduction in crystal length of zeolite crystals reduces deactivation during n-hexane cracking.

$$ln\left(\frac{1}{1-x}\right) = \frac{K\prime\tau\prime}{(1+K_d t^m)} \quad \ldots\ldots. 4.1$$

Where *x* is conversion, K_d is the catalyst deactivation constant (s^{-1}), t is time on stream (min), K' is rate constant (ml/hr*$g_{catalyst}$) , $\tau' = WC_{A0}/F_{A0}$ (W= catalyst

weight in g, C_{A0} = initial concentration in mol/ml and F_{A0} = molar flow rate of reactant in mol/h), t = time on stream in seconds and m is a constant with the value obtained in model as 0.6 (See Appendix D for derivation of Equation 4.1).

Another interesting observation was that the average Propylene to ethylene ratio (P/E) of as-synthesized MTT zeolites was approximately 2.5 after 240 min (see Figure 4.14 and 4.15). High selectivity towards propylene over ethylene displayed by these catalysts possesses interesting shape selectivity properties that attract industries whose target is to increase propylene yield during cracking.

Figure 4.14 Plot of Olefin composition and P/E ratio versus reaction time for S-7-5.

Figure 4.15 Plot of Olefin composition and P/E ratio versus reaction time for S-7-48.

Though the two represented MTT catalysts showed excellent potential as a cracking catalyst, the problem of its fast deactivation when compared to catalyst such ZSM-5 needs to be tackled. One major strategy to tackle deactivation is further reduction in crystal length of particles to very small sizes preferably below the 100 nm range. Microemulsion method [10, 65] is a good technique to achieving this very minute crystal size. Another strategy that may also help in reducing deactivation is the creation of mesoporosity by alkaline treatment [66-68] and or acid leaching [69-71].

4.8 Effect of desilication and mild dealumination of MTT-zeolite

Some of the mechanisms used in minimizing deactivation in zeolites are alkaline treatment or acid leaching. The treatment of catalyst with alkaline preferably NaOH or KOH is also known as desilication. This is because alkaline treatment removes silica from the zeolite frame work thereby creating mesoporosity [72]. However, the removal of silica from the framework of one-dimensional zeolite by desilication leads to blockage of the zeolite micropore by leached framework aluminum [57]. The creation of porosity could thus be maintained by mild acid treatment which removes alumina from zeolite framework thereby creating mesopores in the zeolite framework. Furthermore, our preliminary study also shows that desilication leads to clogging of micropore by alumina.

Desilication followed by mild dealumination of MTT-zeolite sample S-7-48 was carried out as explained in Chapter 3. The desilication process was done for 5 min and 10 min over two different parent sample (S-7-48). This was then followed by mild dealumination. Samples were designated as parent (S-7-48), S-D-5 (Sample desilicated for 5 min) and S-D-10 (Sample desilicated for 10 min).

Figure 4.16 shows the XRD patterns of both parents and desilicated samples. We observe that samples still maintained their crystallinity after the desilication and dealumination process. Though in some instances, crystals of catalyst lose their crystallinity due to excessive desilication [73] or dealumination [71].

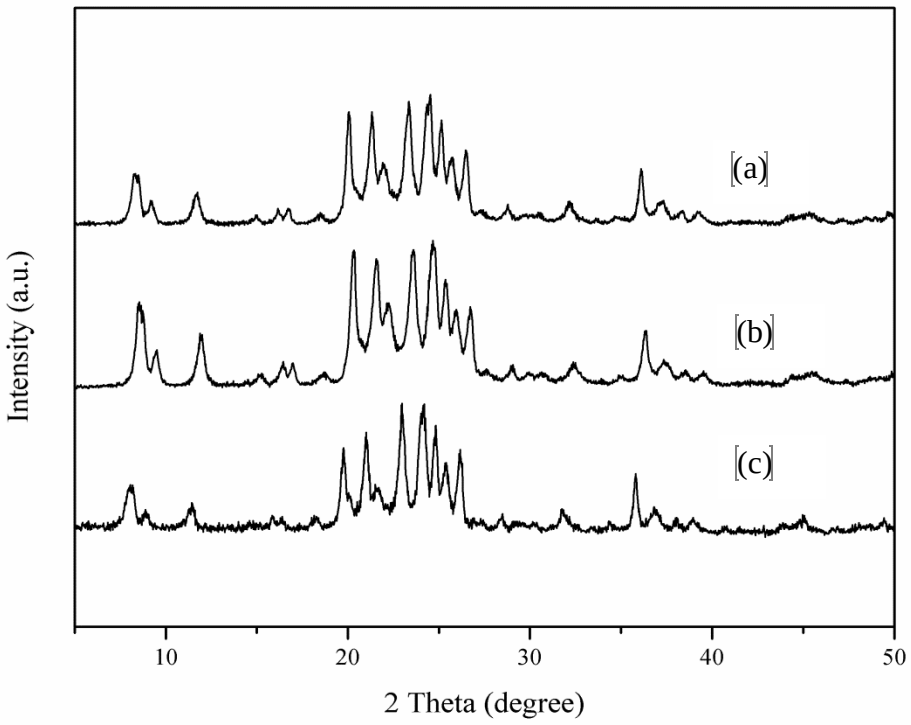

Figure 4.16 XRD pattern of (a) S-D-10 (b) S-D-5 and (c) Parent (S-7-48).

Figure 4.17 shows the FESEM image of sample S-D-5. We further observed that the MTT-type zeolite still exhibits similar rod-like morphology when compared to parent samples as earlier shown in Figure 4.3. However, the existence of extra mesoporosity which is evident in the hierarchical nature of rod-like MTT-zeolite as shown in FESEM image. This hierarchical nature is due to desilication and mild dealumination of samples.

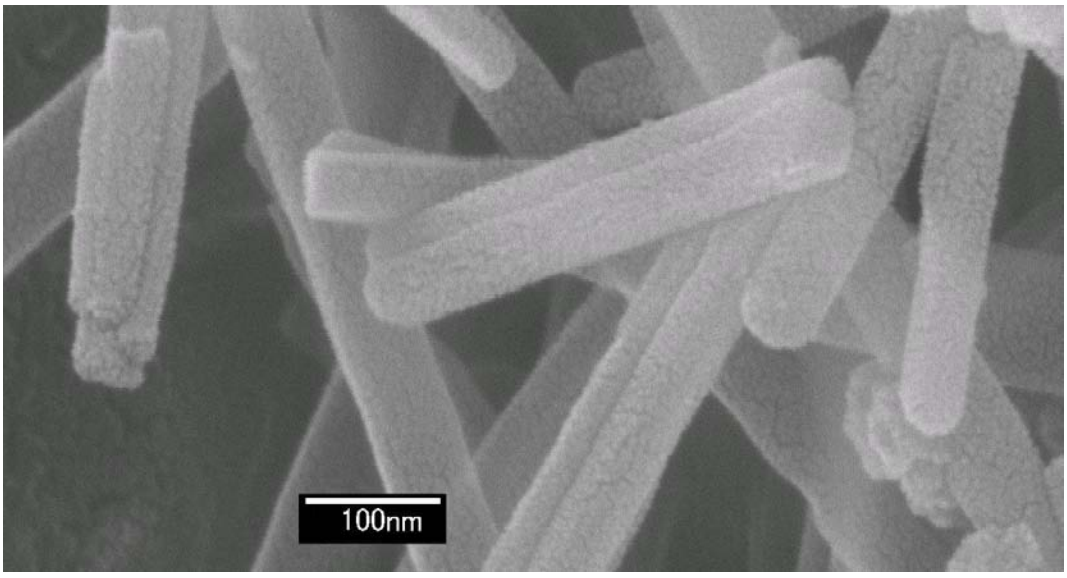

Figure 4.17 FESEM image of sample S-D-5.

Similar hierarchical nature was also observed for sample S-D-10 as shown in Figure 4.18. Furthermore, ^{27}Al NMR of samples S-D-5 and S-D-10 were still consistent with parent sample though with little shift as shown in Figure 4.19. This indicates that Al is located in the tetrahedral position of the zeolite framework.

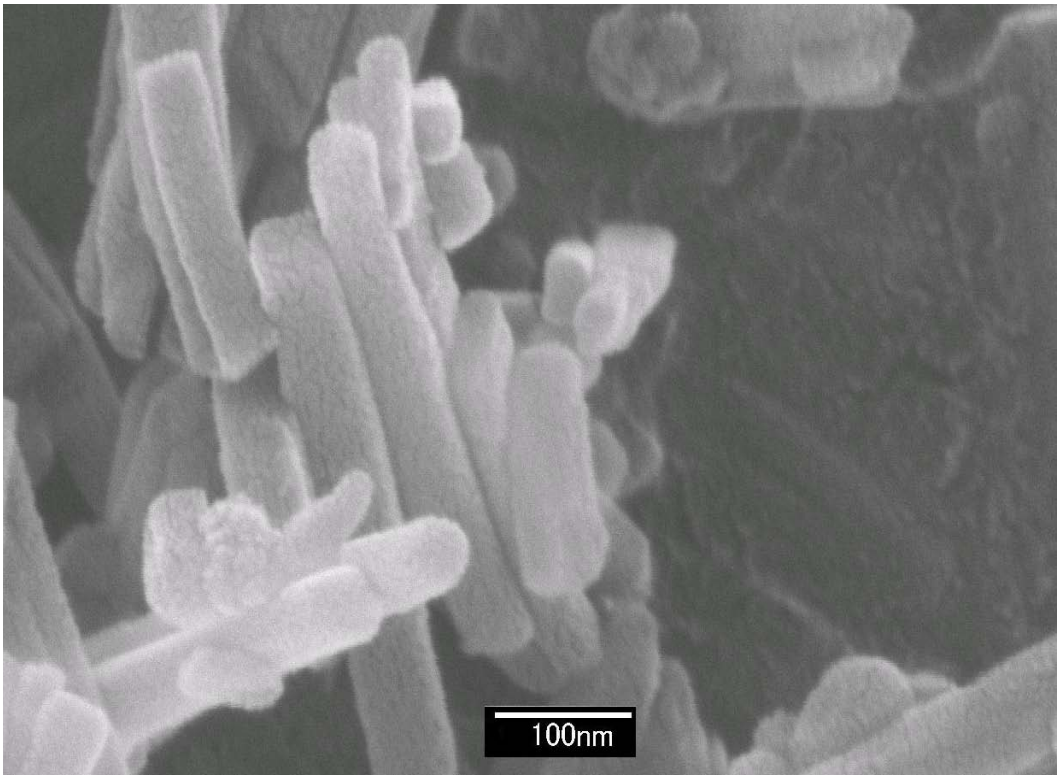

Figure 4.18 FESEM image of sample S-D-10

Si/Al ratio of parent sample and desilicated sample are shown in Table 4.5. We observe a decreasing trend in Si/Al ratio from parent sample (S-7-48) through sample S-D-50 to sample S-D-10. The decrease in Si/Al is evidence to the fact that Si an Al species is being removed from MTT-zeolite framework. A look into the sorption properties of desilicated and dealuminated samples shows improvement in properties of samples when compared to parent sample. As shown in Table 4.6 BET surface area of sample both treated samples were quite greater than that of the parent sample (S-7-48). However, sample S-D-5 shows a more improved BET surface area than sample S-D-10. Desilication time was higher for S-D-10 compared to S-D-5, thus we expect more silica species to be

removed from MTT-zeolite framework. However, as the removal of silica species occur during desilication, freed Al specie in the zeolite framework tend to block the micropore [57]. Therefore, the number of blocked micropore in sample S-D-10 is expected to be more than that in sample S-D-5 due to longer desilication time. For the sake of clarity, let us assume at constant desilication condition, the amount Al species blocking zeolite micropore is ‘n’species/min. For samples S-D-5 and S-D-10, 5n and 10n species are expected to block each samples pore. In order to restore porosity, mild dealumination was done on both samples S-D-5 and S-D-10 for the same microwave resident time. Let assume for this resident time, 3n species of Al were freed from zeolite framework micropore. The amount of Al species left blocking micropores in samples S-D-5 and S-D-10 are 2n and 7n respectively. Thus, we expect more freed pore in sample S-D-5 than sample S-D-10.This is because the amount of Al species blocking the micropore removed is higher for sample S-D-5. Therefore, the BET surface area and micropore Surface area of sample S-D-5 is expected more BET surface area and than that of sample S-D-10.

Table 4.6 Si/Al ratio of parent and desilicated samples.

Samples	Si/Al ratio [a]
Parent (S-7-48)	76
S-D-5	75
S-D-10	66

[a] Measured by X-ray fluorescence spectroscopy (XRF)

Table 4.7 Nitrogen sorption properties of 'Porous' MTT zeolites

Samples	S_{BET} [m^2/g]	S_t [m^2/g]	S_{micro} [m^2/g]	S_{ext} [m^2/g]	V_{total} [m^2/g]	V_{micro} [m^2/g]	V_{meso} [m^2/g]
Parent (S-7-48)	174	130	44	130	0.15	0.065	0.09
S-D-5	310	257	53	231	0.176	0.076	0.10
S-D-10	301	242	68	209	0.199	0.070	0.13

S_{BET}: Surface area by BET method S_t: Surface area by t-plot method

S_{ext}: External surface area by t-plot method S_{micro} :Micropore surface area = S_{BET} - S_{ext}

V_{total}: Volume absorbed at P/Po = 0.98 V_{micro}: Micropore volume by t-plot method

V_{meso} :Mesopore volume = V_{total} - V_{micro}

Furthermore, we observed increasing external surface area and mesoporous area with increasing desilication. This is expected since more Si species are removed with increased extent of desilication.

4.9 Catalytic cracking of n-hexane over hierarchical MTT-zeolite

Catalytic cracking of n-hexane as model reactant was also carried out on samples S-D-5 and S-D-10. Figure 4.19 shows the plot of conversion versus time on stream for parent and desilicated samples. As shown, we observed that the activity rate of desilicated and dealuminated samples (hierarchical samples) is greater than the parent sample. This is because resistance to diffusion is less in treated samples when compared to parent samples. Also, pores formed after alkaline and acid treatment gives better access to more acid sites. This is evident in NH3-TPD of parent sample (S-7-48) and hierarchical sample (S-D-10) as shown in Table 4.7. Our findings agrees with results reported elsewhere [74]. Furthermore, we observed that sample S-D-5 shows the most potential in the cracking of n-hexane. As earlier explained, reduction of deactivation can be achieved via alkaline and or mild acid treatment. We observed that the deactivation rates of treated samples were far smaller compared to parent MTT-zeolite sample. Sample S-D-5 shows the least deactivation rate followed by S-D-10, with the highest being the parent sample (S-7-48).Thus creation of mesoporosity can help create catalyst a more stable catalyst.

Table 4.8 NH3 –TPD of parents and Hierarchical samples

Catalyst	NH_3-TPD ($mmolg^{-1}$)			
	Total acidity	Low temperature L.T. (weak)	High temperature H.T. (medium- strong)	H.T/L.T.
		< 300 °C	300 - 650 °C	
S-7-48	0.267	0.120 (263)	0.147 (470)	1.24
S-D-10	0.297	0.176	0.121	0.688

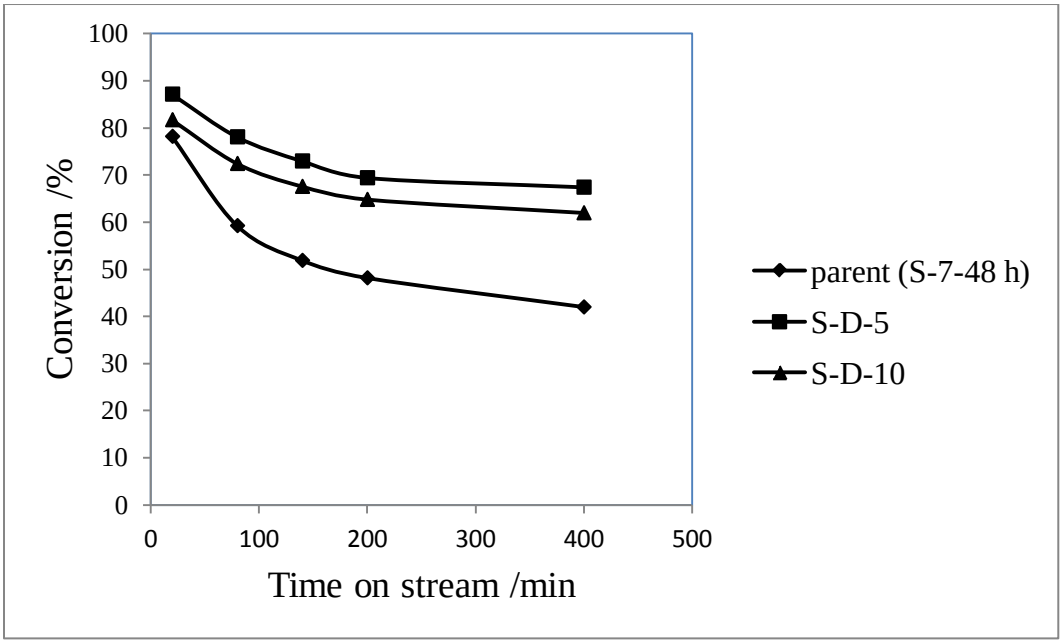

Figure 4.19 Plot of conversion and Time on stream for Parent and desilicated Samples

The average propylene to ethylene ratio (P/E) is ~2.2 and ~2.3 for samples S-D-5 and S-D-10 respectively as shown in Figure 4.20 and 4.21. The average P/E ratio of samples is almost the same with the parent sample which is also ~2.5. The high P/E ratio recorded in these MTT-zeolite samples make them potential

catalysts for selective propylene production. Comparison of P/E ratio of MTT-zeolite with contemporary zeolites as shown in Table 4.8 further emphasizes its potential as a catalyst for selective propylene production.

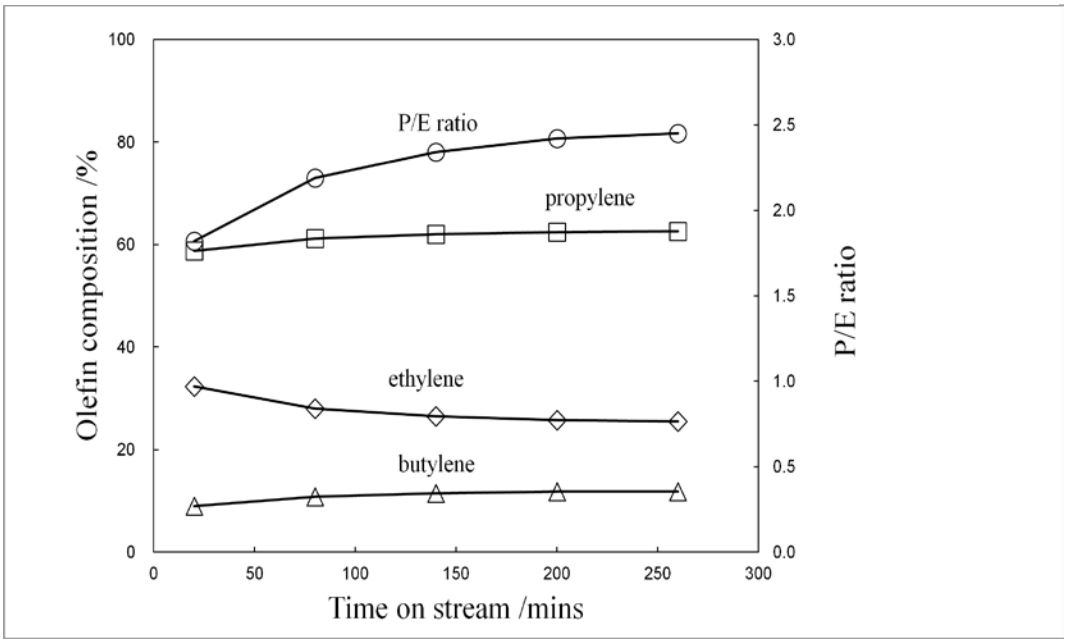

Figure 4.20 Plot of Olefin composition and P/E ratio versus reaction time for S-D-5.

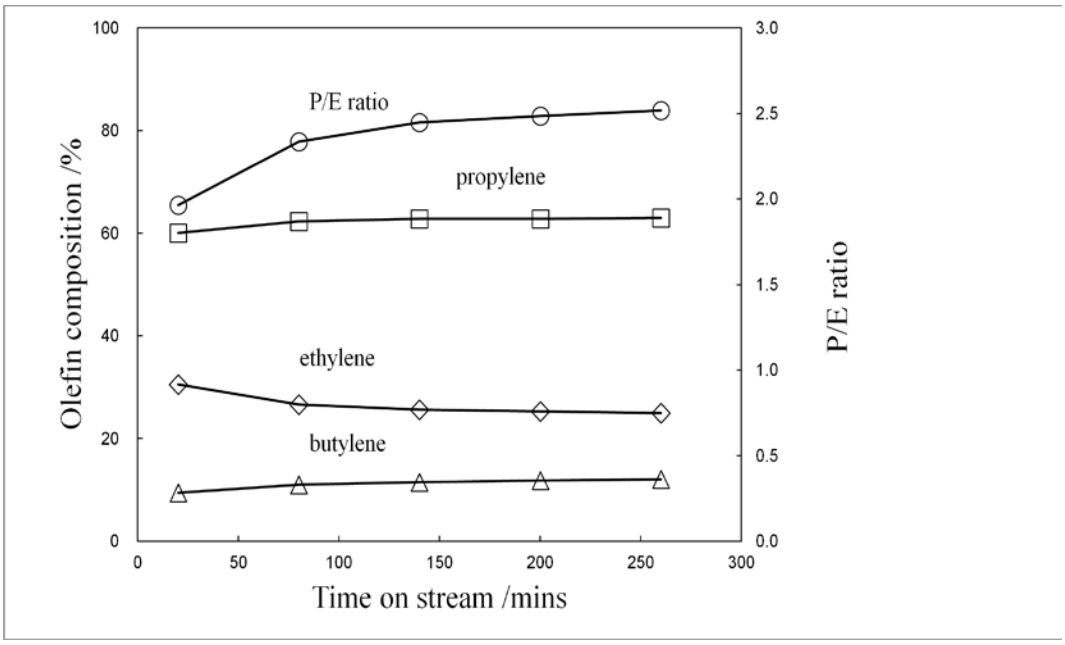

Figure 4.21 Plot of Olefin composition and P/E ratio versus reaction time for S-D-10.

Table 4.9 Conversion and P/E ratio over zeolite samples

Zeolite	Average Conversion	yield/%		P/E ratio	Time on stream	Temperature (^{o}C)	W/F (h)	Reference
		P	E					
ZSM-5	89.87	31.5	17.7	1.8	50 h	650	0.125	[64]
ZSM-5	68.00	32	22.5	1.4	15 h	370	0.333	[50]
MTT (S-D-5)	74.97	26.22	11.9	2.2	4.3 h	650	0.125	This study

Where P=propylene and E=ethylene

CHAPTER 5

CONCLUSION AND RECOMMENDATION

5.1. **Conclusion**: To end with, the two techniques of experimental analysis were used in analyzing the effect of synthesis parameters on properties of as-synthesized MTT zeolite. The analysis results of both techniques pointed in the same direction. It was found that the BET surface area was competitively affected by synthesis parameters in the order: aging time (B) > Brij-78/SiO_2 ratio (A) >interaction (AxB). For the mean crystal lengths of as-synthesized MTT zeolites, synthesis aging time is more significant with minimal competition from Brij-78/SiO2 ratio. The order of significance of synthesis parameters to mean crystal lengths is as thus: aging time (B) >>> Brij-78/SiO2 ratio (A) >interaction (AxB). Protonated samples showed excellent potential in cracking of n-hexane with high P/E ratio of ~2.5 on the average. Deactivation which is common to one-dimensional pore zeolites can be tackled by creating mesopores. Creation of mesoporosity by desilication and mild dealumination increased the catalytic activity and resistance of MTT-zeolite sample to deactivation.

5.2. **Recommendation:** Our study of MTT-zeolite as a potential catalyst for the selective cracking of n-hexane to propylene is of great prospect. In order to achieve a better catalyst and properly understand the activity of our synthesized catalyst we suggest the following points for future studies:

- The effect of SiO_2/Al_2O_3 ratio on the synthesis of MTT zeolite in non-ionic surfactant medium.
- Catalytic cracking of at varying temperatures and W/F values for optimum catalyst condition.
- Catalytic cracking of paraffin over MTT-zeolite using other model compounds, for instance n-heptane.

Appendix

Appendix A: BET analysis of samples

Samples	S_{BET} (m^2/g)	S_{EXT} (m^2/g)	S_{MICRO} (m^2/g)	V_{TOTAL} (cm^3/g)	V_{MICRO} (cm^3/g)
S-0-5	178	55	123	0.149	0.062
S-0-24	210	56	154	0.166	0.078
S-0-48	91	46	44	0.117	0.022
S-4-5	154	47	107	0.137	0.054
S-4-24	182	65	117	0.179	0.059
S-4-48	205	66	139	0.196	0.070
S-7-5	220	89	130	0.199	0.066
S-7-24	162	36	126	0.144	0.063
S-7-48	174	44	130	0.150	0.065

Where S_{BET} = BET surface area, S_{EXT} = external surface area, S_{MICRO}= micropore area, V_{TOTAL} = total volume and V_{MICRO} = micropore volume.

Appendix B: Calculation of mean effect of parameters on BET surface area

Brij-78/SiO_2 ratio (A)	Aging time (B)	Interaction (A x B)	S/N ratio
1	1	1	45.03
1	2	3	46.46
1	3	2	39.14
2	1	3	43.76
2	2	2	45.22
2	3	1	46.24
3	1	2	46.84
3	2	1	44.17
3	3	3	44.82

Mean effect parameters are calculated as thus:

A1 = (45.03 + 46.46 + 39.14)/3 = 43.54 B1 = (45.03 + 43.76 + 46.84)/3 = 45.21

A2 = (43.76 + 45.22 + 46.24)/3 = 45.07 B2 = (46.46 + 45.22 + 44.17)/3 = 45.28

A3 = (46.84 + 44.17 + 44.82)/3 = 45.28 B3 = (39.14 + 46.24 + 44.82)/3 = 43.40

(A x B)1 = (45.03 + 46.24 + 44.17)/3 = 45.15

(A x B)2 = (39.14 + 45.22 + 46.84)/3 = 43.73

(A x B)3 = (46.46 + 43.76 + 44.82)/3 = 45.01

Where: An = mean S/N ratio of Brij-78/SiO_2 ratio at level n (n=1, 2 or 3)

Bn = mean S/N ratio of Aging time at level n (n=1, 2 or 3)

(A x B)n = mean S/N ratio of Interaction at level n (n=1, 2 or 3)

Appendix C

Samples	BET surface area[a] (m^2/g)	S/N ratio BET surface area	Mean crystal length (nm)	S/N ratio mean crystal length	S/N ratio (summation)
S-0-5	178	45.0252	667	-56.4890	-11.4638
S-0-24	210	46.4561	356	-51.0306	-4.5745
S-0-48	91	39.1353	193	-45.7053	-6.57
S-4-5	154	43.7617	467	-53.3819	-9.6202
S-4-24	182	45.2166	407	-52.1891	-6.9725
S-4-48	205	46.2378	367	-51.2847	-5.0469
S-7-5	220	46.8440	737	-57.3484	-10.5044
S-7-24	162	44.1739	409	-52.2375	-8.0636
S-7-48	174	44.8201	322	-50.1476	-5.3275

Appendix D

Integral plug flow equation

$$\frac{W}{F} = \int \frac{dx}{r_A'}$$

1st order reaction rate with respect to reactant hexane

$$r_A' = aK'C_A$$

Deactivate via coking developed by Voorhies (Fogler 4th edition 2006)

$$a = \frac{1}{(1 + K_d t^m)}$$

$$m = 6$$

$$\tau' = W\frac{C_{Ao}}{F_{Ao}}$$

Combinig all the equations give rise to the equation below:

$$\ln\left(\frac{1}{1-x}\right) = \frac{K'\tau'}{(1 + K_d t^{0.6})}$$

References

[1] K. Tanabe, W.F. Hölderich, Industrial application of solid acid–base catalysts, Applied Catalysis A: General, 181 (1999) 399-434.

[2] R. Brzozowski, W. Te¸cza, Shape-selective reactions of naphthalene over zeolites, Applied Catalysis A: General, 166 (1998) 21-27.

[3] D.R. Corbin, M. Keane Jr, L. Abrams, R.D. Farlee, P.E. Bierstedt, T. Bein, Designing zeolite catalysts for shape-selective reactions: Chemical modification of surfaces for improved selectivity to dimethylamine in synthesis from methanol and ammonia, Journal of Catalysis, 124 (1990) 268-280.

[4] E.J. Creyghton, R.S. Downing, Shape-selective hydrogenation and hydrogen transfer reactions over zeolite catalysts, Journal of Molecular Catalysis A: Chemical, 134 (1998) 47-61.

[5] Y. Sugi, Y. Kubota, A. Ito, H. Maekawa, R.K. Ahedi, S. Tawada, S. Watanabe, I. Toyama, C. Asaoka, H.S. Lee, J.H. Kim, G. Seo, Pore structure and shape-selectivity in the isopropylation of biphenyl catalyzed by one-dimensional large pore zeolites, in: M.C. E. van Steen, L.H. Callanan (Eds.) Studies in Surface Science and Catalysis, Elsevier, 2004, pp. 2228-2238.

[6] R. Kumar, P. Ratnasamy, Isomorphous substitution of iron in the framework of zeolite ZSM-23, Journal of Catalysis, 121 (1990) 89-98.

[7] B. Wang, Z. Tian, P. Li, L. Wang, Y. Xu, W. Qu, Y. He, H. Ma, Z. Xu, L. Lin, A novel approach to synthesize ZSM-23 zeolite involving N,N-dimethylformamide, Microporous and Mesoporous Materials, 134 (2010) 203-209.

[8] K. Möller, T. Bein, Crystallization and porosity of ZSM-23, Microporous and Mesoporous Materials, 143 (2011) 253-262.

[9] H. Mochizuki, T. Yokoi, H. Imai, R. Watanabe, S. Namba, J.N. Kondo, T. Tatsumi, Facile control of crystallite size of ZSM-5 catalyst for cracking of hexane, Microporous and Mesoporous Materials, 145 (2011) 165-171.

[10] T. Tago, H. Konno, M. Sakamoto, Y. Nakasaka, T. Masuda, Selective synthesis for light olefins from acetone over ZSM-5 zeolites with nano- and macro-crystal sizes, Applied Catalysis A: General, 403 (2011) 183-191.

[11] A.G. Gomez, G.d. Silveira, H. Doan, C.-H. Cheng, A facile method to tune zeolite L crystals with low aspect ratio, Chemical Communications, 47 (2011) 5876-5878.

[12] K. Iwakai, T. Tago, H. Konno, Y. Nakasaka, T. Masuda, Preparation of nano-crystalline MFI zeolite via hydrothermal synthesis in water/surfactant/organic solvent using fumed silica as the Si source, Microporous and Mesoporous Materials, 141 (2011) 167-174.

[13] http://www.iza-structure.org/databases/.

[14] G.T. Kokotailo, J.L. Schlenker, F.G. Dwyer, E.W. Valyocsik, The framework topology of ZSM-22: A high silica zeolite, Zeolites, 5 (1985) 349-351.

[15] B. Marler, Silica-ZSM-22: synthesis and single crystal structure refinement, Zeolites, 7 (1987) 393-397.

[16] M.A. Asensi, A. Corma, A. Martínez, M. Derewinski, J. Krysciak, S.S. Tamhankar, Isomorphous substitution in ZSM-22 zeolite. The role of zeolite acidity and crystal size during the skeletal isomerization of n-butene, Applied Catalysis A: General, 174 (1998) 163-175.

[17] J.A.M. Arroyo, G.G. Martens, G.F. Froment, G.B. Marin, P.A. Jacobs, J.A. Martens, Hydrocracking and isomerization of n-paraffin mixtures and a hydrotreated gasoil on Pt/ZSM-22: confirmation of pore mouth and key–lock catalysis in liquid phase, Applied Catalysis A: General, 192 (2000) 9-22.

[18] H.M. Aly, M.E. Moustafa, E.A. Abdelrahman, Synthesis of mordenite zeolite in absence of organic template, Advanced Powder Technology.

[19] T. D.B, S. R.V, R. M.I, Development of modified mordenite-zirconia catalysts active at low-temperature in n-butane isomerization, in: P.M. Antoine Gédéon, B. Florence (Eds.) Studies in Surface Science and Catalysis, Elsevier, 2008, pp. 1223-1226.

[20] S.A. Ali, A.M. Aitani, C. Ercan, Y. Wang, S. Al-Khattaf, Conversion of heavy reformate into xylenes over mordenite-based catalysts, Chemical Engineering Research and Design, 89 (2011) 2125-2135.

[21] Z. Zhou, W. Wu, J. Wang, C. Zeng, Tert-butylation of Toluene with Tert-butyl Alcohol over Realuminated H-mordenite Zeolite, Chinese Journal of Chemical Engineering, 17 (2009) 195-199.

[22] E.J.R. Charles J. Plank, Mae K. Rubin, United States Patent 4,076,842, (1978).

[23] W. Huybrechts, J.W. Thybaut, B.R. De Waele, G. Vanbutsele, K.J. Houthoofd, F. Bertinchamps, J.F.M. Denayer, E.M. Gaigneaux, G.B. Marin, G.V. Baron, P.A. Jacobs, J.A. Martens, Bifunctional catalytic isomerization of decane over MTT-type aluminosilicate zeolite crystals with siliceous rim, Journal of Catalysis, 239 (2006) 451-459.

[24] W. Huybrechts, G. Vanbutsele, K.J. Houthoofd, F. Bertinchamps, C.S. Laxmi Narasimhan, E.M. Gaigneaux, J.W. Thybaut, G.B. Marin, J.F.M. Denayer, G.V. Baron,

P.A. Jacobs, J.A. Martens, Skeletal isomerization of octadecane on bifunctional ZSM-23 zeolite catalyst, Catalysis Letters, 100 (2005) 235-242.

[25] R. Kumar, P. Ratnasamy, Isomerization and formation of xylenes over ZSM-22 and ZSM-23 zeolites, Journal of Catalysis, 116 (1989) 440-448.

[26] Y. Liu, Z. Wang, Y. Ling, X. Li, Y. Liu, P. Wu, Synthesis of ZSM-23 Zeolite Using Isopropylamine as Template, Chinese Journal of Catalysis, 30 (2009) 525-530.

[27] B. Wang, Q. Gao, J. Gao, D. Ji, X. Wang, J. Suo, Synthesis, characterization and catalytic C4 alkene cracking properties of zeolite ZSM-23, Applied Catalysis A: General, 274 (2004) 167-172.

[28] D. Ji, B. Wang, G. Qian, Q. Gao, G. Lü, L. Yan, J. Suo, A highly efficient catalytic C4 alkane cracking over zeolite ZSM-23, Catalysis Communications, 6 (2005) 297-300.

[29] N. Kresge; Charles T. (Sewell, McWilliams; John P. (Woodbury, NJ), Vartuli; James C. (West Chester, PA), Nicoletti; Michael P. (Turnersville, NJ), Catalyst for alkylation of aromatic hydrocarbons United states patent 4,547,605, (1985).

[30] M. Gharibeh, G.A. Tompsett, K.S. Yngvesson, W.C. Conner, Microwave synthesis of zeolites: effect of power delivery, J Phys Chem B, 113 (2009) 8930-8940.

[31] A. Arafat, J.C. Jansen, A.R. Ebaid, H. van Bekkum, Microwave preparation of zeolite Y and ZSM-5, Zeolites, 13 (1993) 162-165.

[32] L. Bonaccorsi, E. Proverbio, Influence of process parameters in microwave continuous synthesis of zeolite LTA, Microporous and Mesoporous Materials, 112 (2008) 481-493.

[33] H. Youssef, D. Ibrahim, S. Komarneni, Microwave-assisted versus conventional synthesis of zeolite A from metakaolinite, Microporous and Mesoporous Materials, 115 (2008) 527-534.

[34] M. Sathupunya, E. Gulari, S. Wongkasemjit, Na-A (LTA) zeolite synthesis directly from alumatrane and silatrane by sol-gel microwave techniques, Journal of the European Ceramic Society, 23 (2003) 1293-1303.

[35] D.S. Kim, J.-S. Chang, J.-S. Hwang, S.-E. Park, J.M. Kim, Synthesis of zeolite beta in fluoride media under microwave irradiation, Microporous and Mesoporous Materials, 68 (2004) 77-82.

[36] G. Li, H.-m. Hou, R.-s. Lin, Rapid synthesis of mordenite crystals by microwave heating, Solid State Sciences, 13 (2011) 662-664.

[37] J. Motuzas, A. Julbe, R.D. Noble, C. Guizard, Z.J. Beresnevicius, D. Cot, Rapid synthesis of silicalite-1 seeds by microwave assisted hydrothermal treatment, Microporous and Mesoporous Materials, 80 (2005) 73-83.

[38] H. Liu, G.H. Kuehl, I. Halasz, D.H. Olson, Quantifying the n-hexane cracking activity of Fe- and Al-based acid sites in H-ZSM-5, Journal of Catalysis, 218 (2003) 155-162.

[39] S. Altwasser, C. Welker, Y. Traa, J. Weitkamp, Catalytic cracking of n-octane on small-pore zeolites, Microporous and Mesoporous Materials, 83 (2005) 345-356.

[40] S. Kotrel, H. Knözinger, B.C. Gates, The Haag–Dessau mechanism of protolytic cracking of alkanes, Microporous and Mesoporous Materials, 35–36 (2000) 11-20.

[41] J.H. Lee, S. Kang, Y. Kim, S. Park, New Approach for Kinetic Modeling of Catalytic Cracking of Paraffinic Naphtha, Industrial & Engineering Chemistry Research, 50 (2011) 4264-4279.

[42] F.O. Rice, K.F. Herzfeld, The Thermal Decomposition of Organic Compounds from the Standpoint of Free Radicals. VI. The Mechanism of Some Chain Reactions, Journal of the American Chemical Society, 56 (1934) 284-289.

[43] A. Kossiakoff, F.O. Rice, Thermal Decomposition of Hydrocarbons, Resonance Stabilization and Isomerization of Free Radicals1, Journal of the American Chemical Society, 65 (1943) 590-595.

[44] B.G. Anderson, R.R. Schumacher, R. van Duren, A.P. Singh, R.A. van Santen, An attempt to predict the optimum zeolite-based catalyst for selective cracking of naphtha-range hydrocarbons to light olefins, Journal of Molecular Catalysis A: Chemical, 181 (2002) 291-301.

[45] X. Xian, G. Liu, X. Zhang, L. Wang, Z. Mi, Catalytic cracking of n-dodecane over HZSM-5 zeolite under supercritical conditions: Experiments and kinetics, Chemical Engineering Science, 65 (2010) 5588-5604.

[46] M. Sicard, M. Grill, B. Raepsaet, F. Ser, C. Potvin, G. Djéga-Mariadassou, n-dodecane thermal and catalytic cracking under supercritical conditions, in: P.M. Antoine Gédéon, B. Florence (Eds.) Studies in Surface Science and Catalysis, Elsevier, 2008, pp. 1103-1106.

[47] H. Pan, G. Wei, H. Yuan, Q. Huo, Q. Li, X. Pan, W. Wang, X. Yu, Studies on catalytic cracking catalyst of hydrocarbons with a new type of zeolite L, in: Z.G.J.C.

Ruren Xu, Y. Wenfu (Eds.) Studies in Surface Science and Catalysis, Elsevier, 2007, pp. 1392-1398.

[48] Y. Wei, Z. Liu, G. Wang, Y. Qi, L. Xu, P. Xie, Y. He, Production of light olefins and aromatic hydrocarbons through catalytic cracking of naphtha at lowered temperature, in: N.Ž. J. Čejka, P. Nachtigall (Eds.) Studies in Surface Science and Catalysis, Elsevier, 2005, pp. 1223-1230.

[49] P. Morales-Pacheco, J.M. Domínguez, L. Bucio, F. Alvarez, U. Sedran, M. Falco, Synthesis of FAU(Y)- and MFI(ZSM5)-nanosized crystallites for catalytic cracking of 1,3,5-triisopropylbenzene, Catalysis Today, 166 (2011) 25-38.

[50] A.A. Rownaghi, F. Rezaei, J. Hedlund, Selective formation of light olefin by n-hexane cracking over HZSM-5: Influence of crystal size and acid sites of nano- and micrometer-sized crystals, Chemical Engineering Journal, 191 (2012) 528-533.

[51] S. Ernst, R. Kumar, J. Weitkamp, Synthesis and catalytic properties of zeolite ZSM-23, Catalysis Today, 3 (1988) 1-10.

[52] Y.-D. Chiang, H.-Y. Lian, S.-Y. Leo, S.-G. Wang, Y. Yamauchi, K.C.W. Wu, Controlling Particle Size and Structural Properties of Mesoporous Silica Nanoparticles Using the Taguchi Method, The Journal of Physical Chemistry C, 115 (2011) 13158-13165.

[53] G. Barman, A. Kumar, P. Khare, Removal of Congo Red by Carbonized Low-Cost Adsorbents: Process Parameter Optimization Using a Taguchi Experimental Design, Journal of Chemical & Engineering Data, 56 (2011) 4102-4108.

[54] O.G. Nik, M. Sadrzadeh, S. Kaliaguine, Surface grafting of FAU/EMT zeolite with (3-aminopropyl)methyldiethoxysilane optimized using Taguchi experimental design, Chemical Engineering Research and Design, 90 (2012) 1313-1321.

[55] J.A. Ghani, I.A. Choudhury, H.H. Hassan, Application of Taguchi method in the optimization of end milling parameters, Journal of Materials Processing Technology, 145 (2004) 84-92.

[56] V. Paixão, R. Monteiro, M. Andrade, A. Fernandes, J. Rocha, A.P. Carvalho, A. Martins, Desilication of MOR zeolite: Conventional versus microwave assisted heating, Applied Catalysis A: General, 402 (2011) 59-68.

[57] D. Verboekend, A.M. Chabaneix, K. Thomas, J.-P. Gilson, J. Perez-Ramirez, Mesoporous ZSM-22 zeolite obtained by desilication: peculiarities associated with crystal morphology and aluminium distribution, CrystEngComm, 13 (2011) 3408-3416.

[58] M. Ogura, Y. Kawazu, H. Takahashi, T. Okubo, Aluminosilicate Species in the Hydrogel Phase Formed during the Aging Process for the Crystallization of FAU Zeolite, Chemistry of Materials, 15 (2003) 2661-2667.

[59] O. Larlus, V.P. Valtchev, Crystal Morphology Control of LTL-Type Zeolite Crystals, Chemistry of Materials, 16 (2004) 3381-3389.

[60] T. Tago, D. Aoki, K. Iwakai, T. Masuda, Preparation for Size-Controlled MOR Zeolite Nanocrystal Using Water/Surfactant/Organic Solvent, Top Catal, 52 (2009) 865-871.

[61] Y. Kamimura, K. Itabashi, T. Okubo, Seed-assisted, OSDA-free synthesis of MTW-type zeolite and “Green MTW” from sodium aluminosilicate gel systems, Microporous and Mesoporous Materials, 147 (2012) 149-156.

[62] R. Torkaman, M. Soltanieh, H. Kazemian, Optimization of Parameters for Synthesis of MFI Nanoparticles by Taguchi Robust Design, Chemical Engineering & Technology, 33 (2010) 902-910.

[63] H.S. Fogler, Elements of Chemical Reaction Engineering, fourth ed., Pearson Education, Inc, 2006.

[64] H. Konno, T. Okamura, T. Kawahara, Y. Nakasaka, T. Tago, T. Masuda, Kinetics of n-hexane cracking over ZSM-5 zeolites – Effect of crystal size on effectiveness factor and catalyst lifetime, Chemical Engineering Journal, 207–208 (2012) 490-496.

[65] T. Tago, K. Iwakai, M. Nishi, T. Masuda, Preparation of mono-dispersed MFI-type zeolite nanocrystals via hydrothermal synthesis in a water/surfactant/oil solution, in: I.-S.N. Hyun-Ku Rhee, P. Jong Moon (Eds.) Studies in Surface Science and Catalysis, Elsevier, 2006, pp. 185-188.

[66] F.C. Meunier, D. Verboekend, J.-P. Gilson, J.C. Groen, J. Pérez-Ramírez, Influence of crystal size and probe molecule on diffusion in hierarchical ZSM-5 zeolites prepared by desilication, Microporous and Mesoporous Materials, 148 (2012) 115-121.

[67] K. Sadowska, K. Góra-Marek, M. Drozdek, P. Kuśtrowski, J. Datka, J. Martinez-Triguero, F. Rey, Desilication of highly siliceous zeolite ZSM-5 with NaOH and NaOH/tetrabutylamine hydroxide, Microporous and Mesoporous Materials.

[68] W.C. Yoo, X. Zhang, M. Tsapatsis, A. Stein, Synthesis of mesoporous ZSM-5 zeolites through desilication and re-assembly processes, Microporous and Mesoporous Materials, 149 (2012) 147-157.

[69] B.A. Holmberg, H. Wang, Y. Yan, High silica zeolite Y nanocrystals by dealumination and direct synthesis, Microporous and Mesoporous Materials, 74 (2004) 189-198.

[70] Z. Qin, B. Shen, X. Gao, F. Lin, B. Wang, C. Xu, Mesoporous Y zeolite with homogeneous aluminum distribution obtained by sequential desilication–dealumination and its performance in the catalytic cracking of cumene and 1,3,5-triisopropylbenzene, Journal of Catalysis, 278 (2011) 266-275.

[71] C.S. Triantafillidis, A.G. Vlessidis, L. Nalbandian, N.P. Evmiridis, Effect of the degree and type of the dealumination method on the structural, compositional and acidic characteristics of H-ZSM-5 zeolites, Microporous and Mesoporous Materials, 47 (2001) 369-388.

[72] J.C. Groen, J.A. Moulijn, J. Perez-Ramirez, Desilication: on the controlled generation of mesoporosity in MFI zeolites, Journal of Materials Chemistry, 16 (2006) 2121-2131.

[73] J.C. Groen, S. Abelló, L.A. Villaescusa, J. Pérez-Ramírez, Mesoporous beta zeolite obtained by desilication, Microporous and Mesoporous Materials, 114 (2008) 93-102.

[74] M.S. Holm, S. Svelle, F. Joensen, P. Beato, C.H. Christensen, S. Bordiga, M. Bjørgen, Assessing the acid properties of desilicated ZSM-5 by FTIR using CO and 2,4,6-trimethylpyridine (collidine) as molecular probes, Applied Catalysis A: General, 356 (2009) 23-30.

Vitae

Name	:Idris Akolade Bakare
Nationality	:Nigerian
Date of Birth	:5/23/1985
Email	: alomen2bakare@yahoo.com
Mobile Number	: +996552788647, +2348027057150
Present Address	: Chemical Engineering department, King Fahd University of petroleum, Dhahran, Saudi Arabia.
Permanent Address	33, Abolaji street , Mafoluku Oshodi , Lagos, Nigeria
	:
Academic Background	: Msc Chemical Engineering Dec 2012 king Fahd University of petroleum and minerals, Dhahran, Saudi Arabia. Bsc Chemical Engineering November 2009 Federal University of Technology, Minna, Niger state, Nigeria.